PERFORMANCE OF TIMBER STRINGERS REINFORCED WITH GFRP WRAPS

BY
SARA MARGARITA GÓMEZ CASANOVA

A Thesis
Submitted to the Faculty of Graduate Studies
In Partial Fulfillment of the Requirements
For the Degree of

MASTER OF SCIENCE

Department of Civil Engineering
Faculty of Engineering
University of Manitoba
Winnipeg, Manitoba
Canada

THE UNIVERSITY OF MANITOBA

FACULTY OF GRADUATE STUDIES

*****

COPYRIGHT PERMISSION

Performance of Timber Stringers Reinforced with GFRP Wraps

by

Sara Margarita Gómez Casanova

A Thesis/Practicum submitted to the Faculty of Graduate Studies of The University of Manitoba in partial fulfillment of the requirement of the degree

Of

Master of Science

ABSTRACT

The large amount of timber bridges in North America that are at the end of their service life has driven new attention to the study of effective ways of retrofitting them. Additionally, recent use of fiber-reinforced polymer (FRP) materials in civil engineering applications makes them an interesting alternative for this application because of their lightweight and non-corrosive nature. Glass fibre-reinforced polymer (GFRP) fabrics used for strengthening of aged timber stringers are studied in this research program and compared to GFRP bar systems which have been studied and used successfully in the past for this application. The research program focused on the performance of reinforced stringers containing splits as a result of their aging process.

The research program considered 3 different aspects of the behaviour of aged stringers externally reinforced using GFRP sheets. (1) The effectiveness of different patterns of shear reinforcement on split elements was studied using a direct shear test, (2) the flexural behaviour of reinforced samples was studied using full-scale stringers with dap ends reinforced with GFRP sheets and tested in 3-point bending, and (3) the long term behaviour of the reinforcing system was studied using a durability test.

The shear test used 20 samples to compare three angle configurations, 30°, 45°, and 90° using GFRP sheets and FRP bars in similar reinforcement ratios. The

samples were split artificially, reinforced, and tested in direct shear. The results revealed a better performance of the smaller angle configurations of reinforcement in terms of strength and stiffness. The external reinforcement configurations exhibited higher capacity to resist shear than their bar counterparts. The flexure test on 9 samples was used to analyze the behaviour of full-scale reinforced stringers in terms of mode of failures, rigidity, strength, and strains in the shear reinforcements. Important improvement in strength was achieved compared with reported values of bar-reinforced specimens that used larger amounts of reinforcement. The full-scale beams tested had strong modes of failure which revealed the effectiveness of the external reinforcement to bridge defects in the timber. Finally, observations from the durability test indicate that changes in humidity and temperature could possibly have a negative effect on the bonding properties between the timber and the reinforcement.

Results from this work show the effectiveness of the external reinforcement to retrofit aged timber stringer; additionally, the low variability in results from the bending test on externally reinforced samples gives excellent results in terms of reliability. On the other hand, results from this research program indicate the need to study the long term performance of the reinforcement technique using surface bonded GFRP sheets.

ACKNOWLEDGEMENTS

The author would like to express her appreciation to Dr. Dagmar Svecova, for having had the opportunity to work for her. Her continuous support as well as the contribution of her knowledge and vision made this project possible.

The support of Manitoba Department of Transportation and Government Services is also greatly acknowledged for believing in this project and providing the materials and information essential to its development. The participation of Vector construction Group in the manufacturing of the reinforcement system is also sincerely acknowledged, their availability and technical support were indispensable. The participation and support of ISIS Canada is also greatly appreciated, their vision and enthusiasm in applications of new technology encouraged this project. Special gratitude to Dr. Aftab Mufti for his interest on the project and his valuable suggestions as well as Dr. Darshan Sidhu for his help.

The practical work related to this project was made possible through the collaboration and knowledge of technicians and personnel of the Structures Laboratory at the University of Manitoba. Special thanks are given to Mr. Moray McVey, Mr. Grant Whiteside, Mr. Dino Philopulos, Mr. Chad Klowak, Ms. Evangeline Rivera and Ms. Liting Han. The participation of Mr. Kenton Thiessen in this project is also greatly acknowledged, as well as the assistance of Ms. Irini Akhoukh. Special thanks are given to Mr. Shaun Hay for sharing his knowledge and enthusiasm for this project and for his continuous support.

The author wishes to thank her family for their support and for always believing in her, as well as the support of German Ciro, for his kind enthusiasm and understanding along the development of this project. Thanks are also given to fellow students Mr. Hugues Vogel, Mr. Jeremy Walker, Mr. Carlos Mota, and Mr. Shahryar Davoudi and to all friends.

TABLE OF CONTENTS

LIST OF FIGURES

CHAPTER 2

CHAPTER 3

CHAPTER 4

CHAPTER 5

LIST OF TABLES

LIST OF SYMBOLS

a	=	distance from the end of the split to the reaction on the opposite support
A_B	=	area of the top portion of the split beam
A_T	=	area of the bottom portion of the split beam
b	=	beam width
C	=	compression force acting on the top portion of the split beam
C_A	=	compression force acting on the top portion of the split beam at inner face of shear reinforced portion of the beam
C_F	=	compression force acting on the top portion of the split beam at external face of shear reinforced portion of the beam
d	=	beam depth
kd	=	split height measured from top of the section
E	=	modulus of elasticity of timber
EI	=	rigidity of the element
E_f	=	elastic modulus of reinforcement
F_{fu}	=	ultimate strength of reinforcement
k	=	depth of split measured from top, expressed as a fraction of d
I	=	moment of inertia of the section
I_B	=	moment of inertia of the bottom section of the split beam
I_T	=	moment of inertia of the top section of the split beam

L = span

M_B = moment acting on the middle of the bottom portion of the split beam

M_T = moment acting on the middle of the top portion of the split beam

P = load

q = shear flow

Q = first moment of area of the section

R_1 = reaction at the support opposite to split end

R_2 = reaction at the support at split end

T = tension force acting on the bottom portion of the split beam

V_B = shear force acting on the bottom portion of the split beam

V_T = shear force acting on the top portion of the split beam

z = distance from the face of the shear reinforcement to the end of the split

z_1 = distance from the face of the shear reinforcement until the load point

z_2 = distance from the load point to the end of the split

ε_{fu} = rupture strain of reinforcement

Δ = deflection of a beam measured at midspan

$\Delta\theta$ = change of slope of the deformed curve

ρ = radius of curvature of the deformed section

GLOSSARY

Check – A separation of the wood normally occurring across or through the rings of annual growth as usually as a result of seasoning.

Creosote – A wood preservative that is a distillate of coal tar produced by high-temperature carbonization of bituminous coal.

Dap – A notch cut into the end of a flexural member.

Glued-laminated timber – An engineered product comprised by selected and prepared wood laminations bonded together with adhesives.

Grade – The designation of the material quality of a manufactured piece of wood.

Green wood – Wood freshly cut that has not been dried or seasoned .

Knot – A portion of a branch or limb that has become incorporated in a piece of lumber.

Moisture content – The weight of the water in wood expressed in percentage of the weight of the oven-dry wood.

Pockets – A well-defined opening between the rings of annual growth which develops during the growth of the tree.

Softwoods – Wood from evergreen trees or quick growth.

Split – A separation of the wood through the piece to the opposite surface or to an adjoining surface due to the tearing apart of the wood cells.

Stringer – A structural member that supports the load in the direction perpendicular to its longest dimension.

Timber – Useful construction material produced from logs of trees.

Wane – Bark of lack of wood from any cause, except eased edges, on the edge or corner of a piece of lumber.

Warp – Any deviation from a true or plane surface, including bow, crook, cup or any combination thereof.

Wood – A small, defect-free, piece of material.

CHAPTER 1

INTRODUCTION

1.1 GENERAL

Timber was a very important construction material in North America in the past century at a time of large infrastructure development. As a result, many timber bridges are part of the infrastructure of many regions in Canada. The province of Manitoba owns 725 timber bridges, representing 33% of its bridge infrastructure. Most of the timber brides were constructed from 1950 to 1980; as the expected service life of a timber bridge is about 30 years, most of the bridges are close to the end or already beyond of their service life. The province of Manitoba, as well as many other parts of North America, is facing the challenge to find suitable solutions to extend the service life of its timber bridges due to the prohibitive costs associated with their replacement.

Different materials and techniques have been investigated to find suitable solutions to retrofit timber elements. The development of new materials such as fibre-reinforced polymers (FRP) represents a promising technology for timber strengthening. FRP materials have been successfully used in strengthening of concrete structures for many years. Because or their light weight, that does not

increase the dead weight of the structure after strengthening, these materials are being investigated as a feasible strengthening solution for timber bridges.

1.2 BACKGROUND AND PROBLEM DEFINITION

Many timber bridges in North America have been subjected to harsh weather conditions; aging of their component beams is observed mainly in the form of large splits at the ends that developed along the axis of the elements. The splits make end parts of the beams act as two separate smaller elements which lowers their stiffness and load capacity.

Additionally, since timber bridges were constructed 30 to 50 years ago, higher load capacity requirements have been set in recent years due to the development of heavier trucks. Therefore bridges need to be upgraded to support these new requirements.

A research program has been developed at the University of Manitoba to determine suitable ways to apply the FRP strengthening technology to typical stringers found in the Province of Manitoba bridges. Glass fibre-reinforced polymer (GFRP) bars, in different shear and flexural reinforcement patterns, have been investigated for this purpose (Gentile et al., 2002, Svecova and Eden, 2004, and Amy and Svecova, 2004). These studies have confirmed that using GFRP bars is an effective way to strengthen timber stringers. Some demonstration projects such as the Tourand Creek Bridge (Gentile et al., 2002) also show the

excellent durability performance of GFRP bar reinforced elements after six years of service.

Retrofitting timber stringers using GFRP fabrics is an alternative to bar strengthening. Some advantages of the fabric strengthening process are the lower material costs, easier installation, and the avoidance of drilling holes and grooves. The drilling process used for bar strengthening, leads to concerns about contamination of streams with the wood treatment chemicals. An earlier investigation was completed on full scale beams with GFRP sheets as shear reinforcement only (Hay, 2004). The present investigation refers to the performance of timber beams with shear and flexural reinforcement using GFRP sheets, with a focus on the behaviour of shear reinforcement on split beams.

1.3 OBJECTIVES AND SCOPE

The main objective of this research is to investigate different aspects of the behaviour of timber beams externally reinforced with GFRP sheets. Three different tests have been designed for this purpose: the direct shear test, the bending test, and the durability test. The specific objectives of these tests are:

1. Determine an optimum shear reinforcement pattern to be used for strengthening of full scale beams.

2. Investigate the behaviour and effectiveness of a proposed reinforcement scheme for full-scale stringers using GFRP sheets as flexural reinforcement on tension face of stringers and shear reinforcement as inclined straps at the ends.

3. Determine failure mechanisms and critical cases for the full scale beams reinforced with the proposed scheme.

4. Analyze the behaviour of externally reinforced split timber stringers

5. Make an initial assessment of the durability of the external reinforcement system using GFRP sheets.

The scope of this study is limited to full scale, creosote-treated, aged Douglas-fir stringers. It is limited to short-term behaviour of timber stringers subjected to static loads and for beams reinforced using the proposed reinforcement pattern.

1.4 THESIS ORGANIZATION

The present document is composed of 6 chapters. Chapter 2 is a description of the materials and a summary of the research made in the field of timber strengthening and rehabilitation. It also includes a limited amount of information available regarding to the long-term behaviour and durability of wood adhesives.

Chapter 3 describes the materials used and the test procedures of the three tests included in the experimental program: (1) direct shear test, (2) bending test, and (3) durability test.

Chapter 4 presents the results of the tests. It shows a comparison of performance of the reinforcement patterns on samples subjected to pure shear. It presents the results of the bending test on beams reinforced with the chosen pattern of shear and flexural reinforcement. The results of the bending test were compared with results from previous tests on control beams and shear-only reinforced beams. Finally, the chapter presents the observations made on the test samples subjected to the durability test.

Chapter 5 presents a simplified theoretical model to predict the forces acting on the shear reinforcement straps and compares them with values from measured data. The effect of flexural reinforcement on timber beams have been extensively investigated; the present analysis has been focused on the behaviour of the shear reinforcement and the failure mechanisms of split beams because it is the most critical case.

Chapter 6 presents the conclusions of the current research program. This chapter summarizes the observations made for the three tests done and outlines the advantages of using the proposed reinforcement pattern using FRP sheets in comparison with reinforcement patterns using FRP bars. The chapter also presents conclusions of the analysis made on the capacity of reinforced split

beams and recommendations of further investigation regarding long-term behaviour of the external reinforcement system.

CHAPTER 2

LITERATURE REVIEW

2.1 GENERAL

Timber has been extensively used in the past as a structural material. However with depleting resources, very few new timber structures are currently built. There is a renewed attention in studying its behaviour because of the interest in its rehabilitation. This chapter presents a discussion regarding the materials used in the retrofitting process, a compilation of the related research and other related aspects such as durability of timber.

2.2 STRUCTURAL BEHAVIOUR OF TIMBER

Madsen (1992) defines wood as a small, defect-free piece of material that should be differentiated from timber. Wood strength is constant along the length of the member. In contrast, timber has knots and other natural growth characteristics that make the strength vary along the length of the element. For this reason, timber strength should not be taken as a deterministic number but as a probabilistic quantity. Most research has been carried out on clear wood samples however, this project will investigate the behaviour of timber. The terms wood and

timber may sometimes be used interchangeably, since the term wood is more commonly used.

Wood and timber also have different failure modes. Wood subjected to bending fails in compression by formation of wrinkles in the compression zone while timber fails in tension perpendicular to grain initiated at the vicinity of knot or localized slope of grain.

Design values for timber have been developed in the past based on tests on small scale defect free specimens; this was changed to the in-grade testing approach in the early 1980's. Using this approach, representative samples of full-size elements are tested to obtain more realistic values of timber properties. Allowable stresses are based on a conservative 5^{th} percentile values due to the variability of the material. That means that only 5 % of the samples will fall bellow the allowable stresses.

2.2.1 Bending behaviour of timber

Bending behaviour of timber depends on the ratio of tension to compression strength. Buchanan (1990) described the relationship between bending strength and tension-compression strengths and the size dependent brittle fracture in the tension zone.

A description of the bending behaviour of timber should take into account the linear stress-strain relationship in tension, the nonlinear relationship in compression, the large variability of strength properties, and the influence of size effects. Buchanan explains that bending strength is governed by tension failure for weak boards, but by compression failure for strong boards.

Figure 2.1 shows typical stress-strain relationships for wood depending on the direction of the load, perpendicular or parallel to the grain. Wood in tension has a linear elastic stress strain relationship to maximum load when sudden brittle fracture occurs. In axial compression, wood is more ductile, exhibiting a linear stress-strain relationship up to a certain proportional limit beyond which, ductile yielding takes place producing a long decreasing yield plateau.

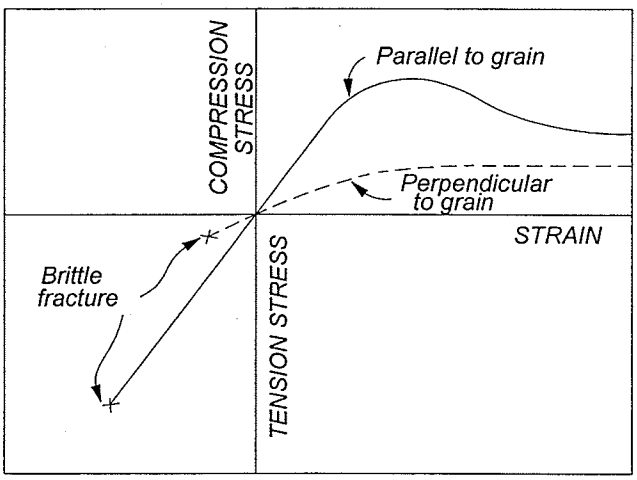

Figure 2.1 Stress-strain relationships for wood (Buchanan, 1990)

The behaviour of wood in bending depends on the relative values of tension and compression strengths. There are four possible modes of failure: (1) for materials with lower failure stress in tension than the proportional limit stress in compression, failure is produced by brittle fracture in the tension zone without

compression yielding. This behaviour is characteristic of weak pieces of commercial lumber. (2) For intermediate ratio of tension to compression strength, some compression yielding occurs which makes the neutral axis shift toward the tension zone until failure is produced by rupture in the tension zone. This is characteristic of stronger pieces of commercial lumber. (3) For a material considerably stronger in tension than in compression, bending is governed by compression behaviour alone. A significant compression yielding occurs and tension stresses continue increasing until rupture occurs in the tension zone at a moment below peak moment. (4) For a material that is much stronger in tension than in compression, maximum moment is associated with compression yielding with no tension failure. This is the behaviour of a green branch in which a plastic hinge forms but it doesn't break. The bilinear stress-strain relationship of timber in compression was analyzed by Buchanan based on previous work described by Bazan (1980). The stress-strain relationship proposed by Bazan can be seen in Figure 2.2.

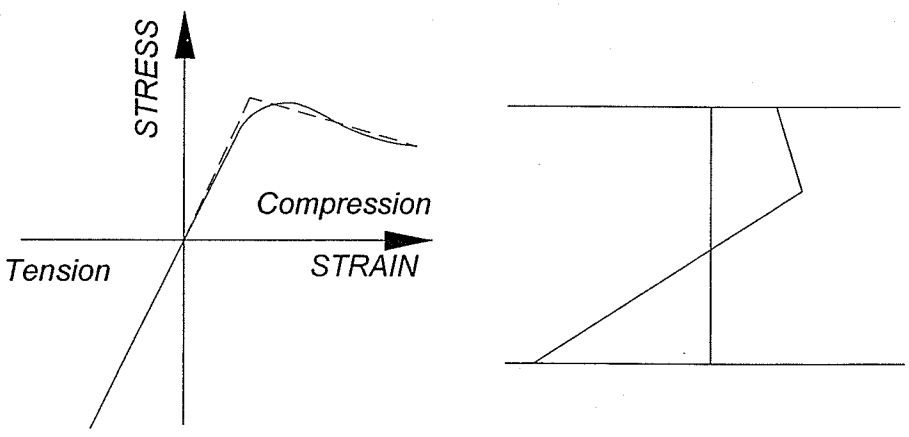

(a) Stress - strain relationship *(b) Stress distribution*

Figure 2.2 Stress distribution proposed by Bazan (1980)

When analyzing ultimate strength model for lumber it is important to take into account the effect of member size. The size effect is a statistical phenomenon related to brittle fracture in the tension zone as proposed by Weibull (1939). Using the description above, Buchanan proposed a strength theory which includes the nonlinear compression behaviour and size-dependant brittle tension behaviour of wood.

2.2.2 Shear behaviour of timber

Shear design values for timber are currently based on small defect-free, straight-grain ASTM shear block test. Effects of member size on shear strength have been addressed by various authors. Huggins et al. (1964) found that shear strength depends on the shear span. Foschi and Barrett (1976, 1977) studied shear strength with Weibull's weak link theory; they found that shear strength varies with beam geometry and loading. This work is the basis of the size effect relationships in the Canadian building code.

Some authors have investigated shear strength of unchecked un-split timber beams (Rammer et al., 1996, Leicester and Breitinger, 1992). Under service conditions, timber beams tend to develop checks and splits as a result of moisture variation; that changes the behaviour of an element in shear. The effects of splits and checks on residual shear strength have also been studied. Markwardt (1931), and Cline and Heim (1912) studied different classes of wood and observed larger incidence in shear failures for air-dried elements over green

elements; they also observed that as specimen size decreases, percentage of shear failures decreases too.

Newlin et al. (1934) proposed a theory to explain the effect of checks and splits and conducted bending tests on build-up beams. Their theory is incorporated into current design standards. This theory is known as the two-beam theory; the length and position of the split is not considered in this theory, only the position of the load from the support, the span, and depth of the beam. However researchers have shown that the underlying assumptions of this theory are incorrect (Keenan 1974, Soltis and Gerhardt 1988). Norris and Erickson (1951) studied the effect of splits on shear strength of timber beams. They determined empirically a stress concentration at the tip of the split in terms of the split length to beam depth ratio.

Huggins et al. (1966) studied the effect of delamination for glued-laminated timber. After testing 175 small glued-laminated beams some of them with simulated splits or delaminations, they concluded that shear span influences strength and delamination reduces ultimate strength. Additionally, they found that shear strength decreases under repeated loading.

2.3 FRP MATERIALS

Fibre-reinforced polymer (FRP) materials have been used in the aeronautical, aerospace and other fields for decades; they have been used in civil engineering

for structural use more recently. FRP products are up to six times stronger than steel and one fifth its weight, and they are non corrosive materials. These characteristics have made FRP materials a good alternative for reinforcement over steel mainly because steel can corrode when subjected to harsh environments. They are fabricated in different forms such as bars, fabrics, 2D grids, 3D grids, or standard structural shapes. The availability of FRP products in the form of thin sheets and laminates are an attractive, economical solution for strengthening of existing structures made of various materials. FRP retrofitting and strengthening methods are gaining wide acceptance as effective and economic infrastructure rehabilitation technologies (ISIS Canada, 2001).

FRPs are composite materials formed by high resistance fibres embedded in a polymeric matrix. The fibres provide their strength to the material while the matrix provide protection to the fibres.

Fibres have high strength and stiffness; their performance is affected by their length, cross-sectional shape and chemical composition. According to ISIS Canada (2001), the most commonly used fibres are carbon, glass and aramid. The polymeric matrix is the material that coats the fibres, protects them from mechanical abrasion, transfers stresses between them, and provides lateral support against bucking. It also transfers inter laminar and in plane shear stresses. The matrix is formed by resins; polyester, vinilester and epoxy are the most commonly used. Additives are a third component of FRP materials. They are used to reduce cost, reduce shrinkage, improve smoke performance,

increase weather resistance, increase stiffness, and improve crack initiation and crack propagation. The most used ones are calcium carbonate, kaolin, silica and talc.

Mechanical properties of FRP products depend on fibre quality, fibre orientation, shape, volumetric ratio, type of matrix, adhesion to the matrix and manufacturing process. There is a wide variety of FRP products using different fibres, matrices and forms, a comparison between some of them is shown in Figure 2.3.

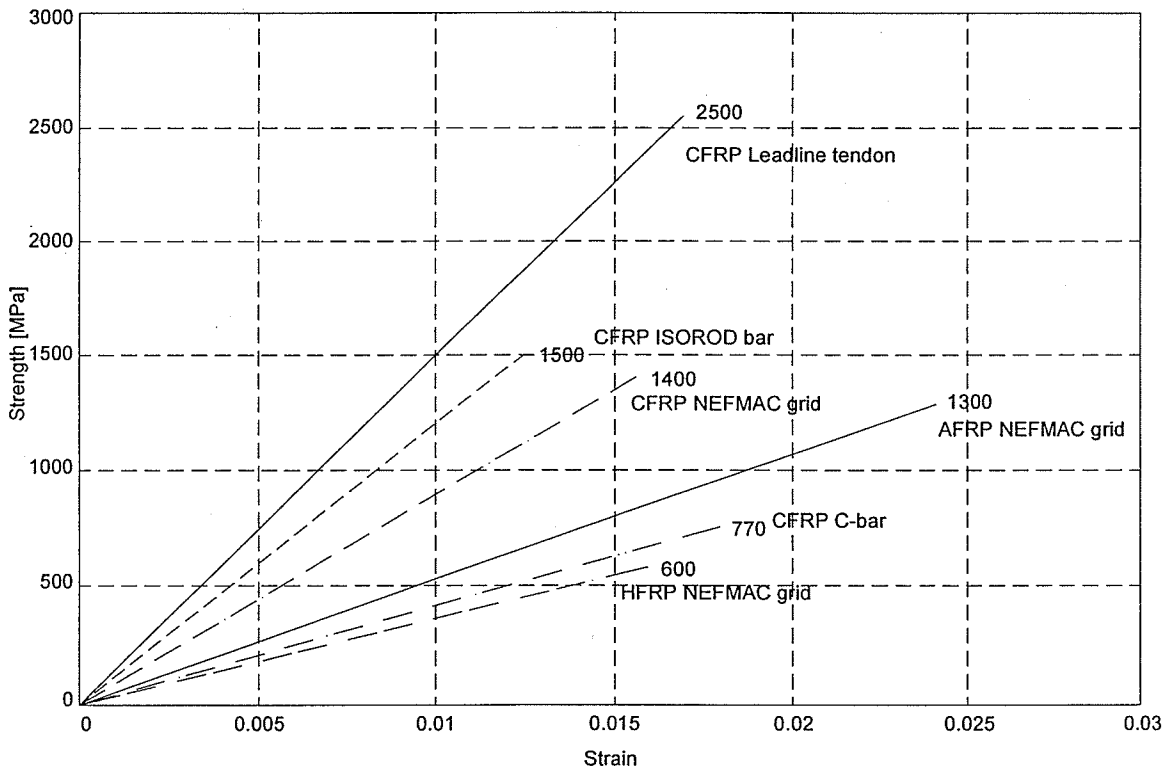

Figure 2.3 Stress-strain relationships of FRP materials (ISIS, 2001)

2.4 BEHAVIOUR OF STRENGTHENED TIMBER

2.4.1 Bending behaviour of strengthened timber

The behaviour of wood members reinforced with FRP sheets has been previously addressed by various authors. Plevris and Triantafillou (1992) and Triantafillou (1997) investigated the effect of FRP fabrics as external bending and external shear reinforcement, respectively. Their analytical work predicted the effect of different reinforcement ratios on the modes of failure and bending capacity of reinforced elements as well as the contribution of FRP reinforcement to shear capacity. Reinforcement patterns with fibres oriented in the longitudinal direction exhibited optimal results for shear-reinforced specimens. Their predictions based on analytical work were in good agreement with results from tests on 30 x 51 x 760 mm and 65 x 100 x 600 mm defect-free samples; their work provided basic understanding of the behaviour of reinforced wood elements.

Reinforcement layers of FRP fabrics on the tension face of small samples have been studied by various authors. Johns and Lacroix (2000) compared tests on 39 x 89 x 1675 mm samples reinforced with different patterns of FRP fabric reinforcement. They reported strength increases larger than values predicted using simple transformed-section analysis. They observed that the reinforcement bridges local defects increasing the strength of the wood itself. Abdel-Magid et al. (1994) reported the superior performance of the wet fabrication technique over the preimpregnated fabrication technique. In the wet fabrication technique, the

reinforcement is fabricated and simultaneously bonded to the timber surface; in the other technique, preinpregnated reinforcement is heated to make resin flow and then bonded to the surface of timber. Comparison of these techniques and different kinds of reinforcement on tension face of beams were studied by testing 38 x 89 x1219 mm Hemlock samples. The authors observed that low volume fractions of carbon fiber reinforcement produce significant increase in modulus of elasticity and capacity of reinforced elements and also lead to more ductile compressive failures. Chen and Balaguru (2003) created a design procedure for estimation of FRP area required to resist increasing loads based on an analytical approach that combines the linear elastic behaviour of reinforcement with the linear-elastic behaviour of wood in tension and elasto-plastic behaviour of wood in compression. Their model is based on mechanical properties of clear wood specimens available from the Wood Handbook and produced reasonably accurate results compared with experimental results.

2.4.2 Retrofitting of old timber beams

Gentile et al. (2002) tested half-scale and full scale timber beams strengthened with near-surface GFRP bars with reinforcement ratios ranging from 0.27 to 0.82%. Test samples were obtained from dismantled bridges that have been in service over 30 years. They reported increases in strength ranging from 18 to 46% and observed that the reinforcement changes the mode of failure from brittle tension to ductile compression. Their analytical model was based on a modification of the work by Buchanan (1990) and it successfully predicts the

flexural capacity of reinforced and unreinforced beams. Svecova and Eden (2004) carried out static tests on 100 x 300 x 2000 mm beams reinforced for flexure and shear with different combinations of FRP bars. Neither shear-only nor flexure-only reinforcement patterns prevented simple tension failure or tension crack propagation. The optimal reinforcement scheme was obtained by a combination of bending reinforcement on tension face and shear reinforcement as vertical dowels spaced at a distance equal to the beam depth. The authors concluded that this strengthening scheme bridges the discontinuities through the entire length of the beam where load is transferred to the GFRP reinforcement after timber had cracked producing compression failures of the strengthened elements. Amy and Svecova (2004) studied bar reinforcement schemes on full-size 100 mm x 400 mm x 3400 mm salvaged dapped stringers. They compared flexure-only reinforced beams with beams with a combination of flexure and shear reinforcement introducing dowel bars at an angle of 60°. The authors found no appreciable increase in mean ultimate load for flexure-only strengthened stringers where dap failures and horizontal shear failures were typical. Beams reinforced for both shear and flexure obtained a mean increase of 22% in the ultimate load compared with control stringers; the shear dowels prevented shear and dap failures in most cases avoiding propagation of existing horizontal splits. Hay et al. (2005) compared the performance of diagonal versus vertical shear reinforcement with GFRP fabric sheets bonded externally to the vertical faces of stringers at the ends. Their work concluded that diagonal reinforcement successfully increases strength and stiffness of the stringers but vertical GFRP sheets were less effective.

2.5 DURABILITY OF STRENGTHENED TIMBER

Fibre-reinforced polymers (FRP) have recently gained attention for having the potential of use to reinforce wood-based materials. However, there is a concern regarding the susceptibility of the bond of FRP-wood interfaces and long term performance of strengthened structures.

2.5.1 Accelerated aging tests

Prediction of the aging behaviour of wood products exposed to the environment is very difficult due to the variability of the different factors such as humidity, temperature and weather conditions. These factors are too random to be analyzed statistically because they never repeat any cycles or patterns. A given combination of factors would be characteristic of a certain location and the solution could not be general. The alternation of climatic conditions such as dampness and dryness produce swelling and shrinkage that affect the internal structure of wood-based products, thus causing strength losses. Long term behaviour of wood-based composite materials has to be investigated using short-term laboratory tests. The attempts to simulate long-term exposure of materials are called accelerated aging tests; they are used to determine, within a short period of time, the suitability of a material for application under severe climatic conditions. Accelerated tests have to impose severe conditions to account for the shorter time of exposure as compared to natural aging. A number of test methods have been developed to evaluate the suitability of adhesives for different wood

applications and to predict the performance of glued products. For given exposure conditions, test results are generally evaluated through different parameters such as delamination (glue line opening right after testing) and strength loss after exposure tests (either wet or dry, after reconditioning to standard moisture content).

The most common used standards to test adhesives for wood are ASTM D3434, ASTM D2559, and ASTM D1037. ASTM D3434 (1996) is used, for comparison of long-term durability between different adhesives. The specimens are subjected to cycles of submerging in boiling water and drying; afterwards, they are tested in tensile shear in the wet phase and the dry phase. In ASTM D2559 (1999), cycles of moisture between 12 and 100% and temperatures of 22°, 65°, and 100°C are administered along with vacuum-pressure change from -85 to 517 kPa and then to zero applied pressure. After the cycles, the percentage of delamination at the bondline is measured and compared. This test is used to evaluate the resistance to delamination of a six-level stair laminated wood sample. ASTM D1037 (1999) uses six cycles of boiling to freezing temperatures and 10 to 100% humidity. After the cycles, different properties of the panels are evaluated to compare before and after the test; the most commonly used are the compression block shear test and the internal bond test. This test is largely applied in North America for evaluating properties of fiber and particle-based panels.

Deppe (1981) presents the XENOTEST process in an attempt to simulate the conditions of exterior exposure as closely as possible. The program was based

on 100-year long list of climatic data from central Europe. It contains different parameters including global irradiation as well as fog and frost effects and the evaluation criterion used is tensile strength. The author reports good agreement between results of exterior exposure and XENOTEST. Approximately 24 weeks of XENOTEST exposure represents, according to the author, five years of exterior exposure, and 48 to 60 weeks represent about 10 years of exterior exposure.

2.5.2 Current research using accelerated aging tests

Current ASTM standards have been used by many researchers to characterize the behaviour of wood-glued products mostly comparing different types of glues, manufactured products or factors in the manufacturing process. Scoville (2001) and Okkonen and River (1996) used ASTM D1037 standard to compare 2 different adhesives and 4 commercially available wood-based products respectively. FRP-wood composite products have also been analyzed using accelerated aging methods mostly to compare different adhesives. Lopez-Anido et al. (2000) used five cycles of accelerated exposure from ASTM D1101 (Method B) to compare the effect of accelerated tests on two types of resins, vinyl ester and phenol resorcinol formaldehyde (PRF). They used samples of hybrid composites of eastern hemlock glulam panels reinforced with E-glass face sheets. Davalos et al. (2000) compared durability and shear strength of two types of bonds (phenolic and epoxy FRP-wood) using modified ASTM D2559 to study

and select better parameters for fabrication, and ASTM D905 shear block test was used to compare the two products.

In general, researchers conclude that performance evaluation tests are very useful for comparison but not sufficient to predict whether or not bonded interfaces will delaminate under general moisture, temperature and service load (Davalos et al. 2000, Deppe. 1981). Ideally, long-term exposures should be conducted to correlate with short-term accelerated tests to validate them. It is not known how to expose a specimen in a laboratory so that results can be extrapolated into long-term natural exposure. Long-term outdoor exposure will take many years to perform and the results will be characteristic of a specific climate. Deppe (1981) concluded that from practical knowledge presently available, considerable differences exist between the results from the exterior exposure and the so called accelerated aging tests. They were found to be too severe and occasionally one-sided in their results, as they are for specific adhesives and therefore cannot give results independent of the adhesives used. The reproducibility of exterior exposures leaves much to be desired due to the influence of macro- and micro- climatic factors. Another problem is that on site application of adhesives is a delicate job, and properties of reinforced elements very much depend on the workmanship. Many factors are likely to affect bond properties (wood surface preparation, moisture content gradients, adhesive thickness or environmental conditions); they are difficult to simulate in standard test procedures.

Raknes (1997) tested eight urea-formaldehyde (UF) glues and one acid-phenolic (PF) glue for long-term durability, and compared them with "established" glues of the resorcinol (RF) types. The author used accelerated and natural aging and compared results after 30 years. The accelerated aging was investigated with testing pieces made from 18 x 1in glued with 1in overlap and tested by tension shear. Three sets of tests were made for three different exposures: (1) Standard atmosphere (20°C, 65% R.H.), during 5 years, (2) cycling between 20-25°C, 85-90% R.H., and 50°C, 50-60% R.H., periods of 1 month during 3 years, and (3) Cycling between 20-25°C, 85-90% R.H., and 25-30°C, 25-30% R.H., for periods of 1 month during 5 years.

Natural aging was investigated using test blocks 15 cm x 15 cm x 30 cm consisting of six laminations cut from laminated beams of spruce. The sample blocks were stored under 5 different conditions: (1) standard atmosphere, 20°C, 65% R.H., (2) outdoors, protected by roof, (3) unheated, ventilated loft with an estimate range of temperature and humidity of 10 to 35°C, 40 to 80% R.H., (4) In a heated cellar, with rather dry atmosphere for an estimated range of 15 to 25°C, 30 to 60% R.H., (5) Outdoors unprotected on a roof. Samples were removed at intervals and tested according to ASTM 1059, and ASTM D 905. Outdoor exposure was interrupted after 10 years and indoor and protected outdoor exposure after 22 years.

Results correlated quite well giving good values of dry strength in both exposure types for Caseins, Resorcinol (RF) and phenol-resorcinol (PRF); and urea-

formaldehyde (UF) glues retained their dry strength in natural indoor exposures and reasonably well in accelerated exposures. Acid PF gave mostly poor results in all exposures. The authors concluded, based on these results, that a suitable temperature-humidity cycling will give valuable information about the long-term durability of adhesives.

CHAPTER 3

EXPERIMENTAL PROGRAM

3.1 GENERAL

The experimental program was completed in the McQuade Structures Laboratory at the University of Manitoba. Three types of tests were carried out. (1) Direct shear test on small specimens reinforced with different GFRP materials and patterns, (2) 3-point bending test of full scale stringers reinforced with GFRP wraps for bending and shear, and (3) durability test on full scale beams subjected to cycling changes of temperature and relative humidity. The tests were designed to evaluate different aspects of the performance of timber beams retrofitted using GFRP sheets.

3.2 MATERIALS

3.2.1 Timber

The timber used for all tests was Douglas Fir taken from 30 to 40 years old dismantled bridges. Creosote treated timber was used for bending and durability tests while non-treated timber was used for the shear test.

Douglas-fir is recognized among the softwoods as one with the best strength-to-weight ratio and the highest rates of extreme fibre stress in tension, tension parallel-to-grain and compression perpendicular-to-grain. It has also one of the highest values of modulus of elasticity which is a parameter that describes the rigidity of an element.

3.2.2 Strengthening systems

Two strengthening systems were used in this research program: GFRP sheets and GFRP bars. GFRP sheets were used as external reinforcement in this experimental program. The reinforcement system used in the tests is a commercial brand, Wabo ®MBrace system. It has been mostly used for retrofitting concrete structures in the past. In earlier tests (Hay, 2004), it has demonstrated a good performance when used for the strengthening of timber stringers. The system combines E-Glass unidirectional fibre fabric - Wabo®MBrace EG900 - saturated in an epoxy matrix - Wabo®MBrace Saturant. The glass fibre composite is a lightweight reinforcement with good corrosion resistance and it is a cost effective alternative that provides strength and good long term performance to the strengthened elements. A third component of the system - Wabo®MBrace Primer - is applied to prepare the surfaces for application of saturant to guarantee a good bonding between the base material and the reinforcement. Properties of the three components are shown in Table 3.1. These values are given by the manufacturer and are used in analysis and design. The reported values are

obtained by testing cured laminates and divide the resulting strength and modulus values by the nominal fabric thickness.

Table 3.1 Tensile properties of Wabo®MBrace system components.

	Ultimate Strength, F_{fu} [MPa]	Elastic Modulus, E_f [GPa]	Rupture Strain, ε_{fu} %
Wabo ®MBrace EG900	1517.0	72.4	2.1
Wabo ®MBrace Saturant	55.2	3.0	3.5
Wabo ®MBrace Primer	14.5	0.71	40.0

GFRP bars with 9 millimeter diameter were used as shear reinforcement in one type of the shear test samples. The dowels used in this test were Aslan 100-101 GFRP bars with a tensile strength of 760 MPa and shear strength of 152 MPa. The bar properties are shown in Table 3.2.

Table 3.2 Physical properties of Aslan 100-101 GFRP bars.

	Diameter [mm]	Area [mm^2]	Nominal Diameter [mm]	Tensile Modulus [GPa]	Tensile Strength [MPa]	shear Strength [MPa]
#3	9 mm	84.32	9.53	40.8	760	152

3.3 SHEAR TEST

The purpose of this test was to evaluate the performance of different shear reinforcement schemes for split beams. Shear strength of small clear specimens

should be tested following guidelines of ASTM D905 (1998). The purpose of this test could not be attained with the use of small specimens, therefore a special setup was designed for this test. The specimens were obtained by cutting old Douglas-fir beams into 75 mm x 190 mm x 774 mm pieces. Each specimen was cut longitudinally to make an artificial split and then reinforced and tested in direct shear.

3.3.1 Test specimens

The test specimens were cut from old beams without creosote treatment; the beams were provided by the Manitoba Department of Transportation and Government Services. The original beams had checks and splits that developed over years of service. The test specimens were cut from the beams using portions of the available material without significant damage.

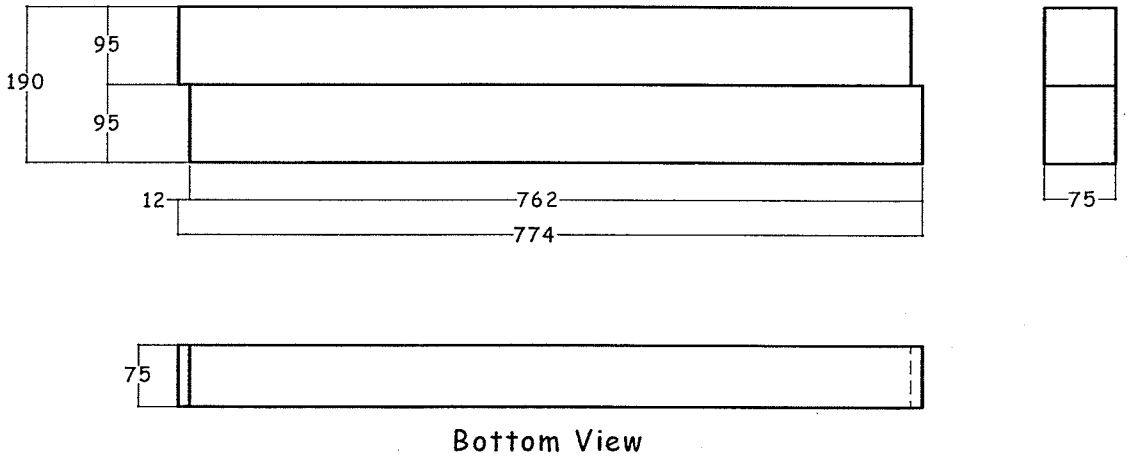

Figure 3.1 Test specimens for shear test

All the tested samples were 190 mm X 75 mm X 774 mm. They were cut into two identical portions of 95 mm X 75 mm X 774 mm. A small wedge was cut at opposite edges of each portion. This groove made the sample fit in the testing frame. A sketch of the test samples is shown in Figure 3.1. A total of 20 identical specimens were reinforced using 5 different strengthening schemes.

Twelve specimens were tested in direct shear using bar reinforcement. Four specimens had a dowel bar aligned at 30°. The reinforcement ratio for this scheme was 0.3%. Four specimens had a dowel aligned at 45°. The reinforcement ratio for this scheme was 0.21%. The final four specimens had two dowels aligned at 90°. The reinforcement ratio for this scheme was 0.3%. The reinforcing schemes using GFRP bars are shown in Figure 3.2.

Two reinforcing schemes using GFRP sheets were tested using 4 test specimens for each pattern, for a total of 8 specimens. The first scheme was formed by 1 ply of sheet 125 mm wide inclined at 45° from longitudinal axis and wrapped to one face of the wood. The resulting reinforcement ratio for this scheme was 0.21%. The second scheme was reinforced using 1 ply of sheet 125 mm wide inclined at 30° from longitudinal axis and also wrapped to one face of the wood for a reinforcement ratio of 0.30%. A sketch showing the sheet reinforcing patterns is shown in Figure 3.3.

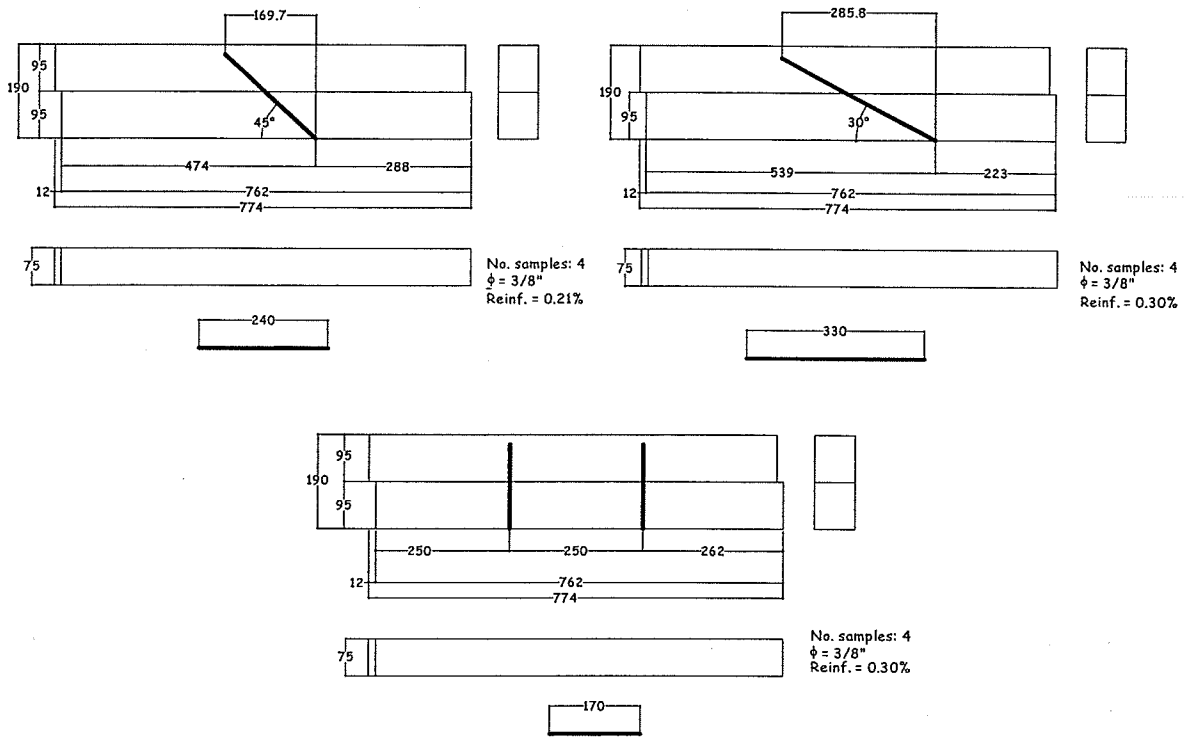

Figure 3.2 Reinforcement scheme for shear test using GFRP bars

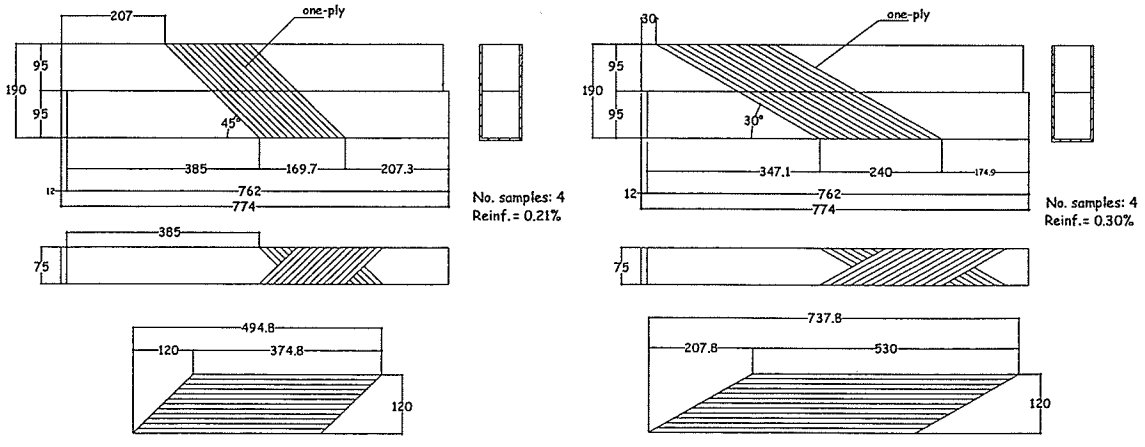

Figure 3.3 Reinforcement scheme for shear test using GFRP sheets

3.3.2 Fabrication of samples and strengthening procedure

The samples were brought to Vector Construction Ltd. for strengthening. Before strengthening, the samples were split in the middle as discussed earlier and the two parts belonging to the same original piece were strongly tied mechanically using provisional metallic straps. Small pieces of material were used to protect the samples avoiding crushing of wood fibres under the straps, as shown in Figure 3.4.

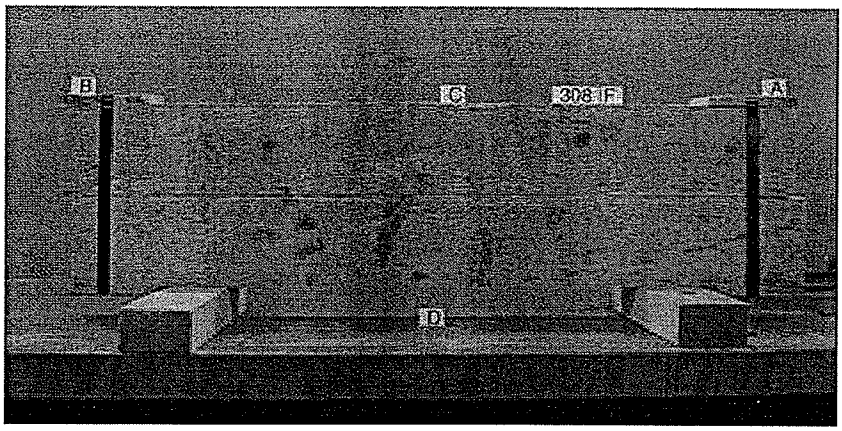

Figure 3.4 Test specimens for shear test

For bar reinforced specimens, dowel holes were drilled at 90°, 45° and 30° angles. Caulking was placed around the shear plane of the sample to prevent epoxy from spreading into the shear plane and cracks of the sample. Epoxy was then poured into the drilled hole and the GFRP dowels were inserted immediately. The insertion of the dowels is displayed in Figure 3.5.

For GFRP sheet strengthened specimens, the edges of the elements were rounded to allow full contact between the wood and the reinforcing sheet at

places where the reinforcement is wrapped. The strengthening process began with cleaning the surface of the beams with a soft brush while the dust was vacuumed. After the surface was cleaned, a layer of primer was applied with a short nap roller as shown in Figure 3.6. Following primer application, the first layer of epoxy saturant was applied to the timber surface and a piece of FRP sheet was placed on the saturant and pressed against the surface using a metallic grooved roller as shown in Figures 3.7, 3.8 and 3.9. To complete the process, a second coat of saturant was applied. This step of the process is shown in Figure 3.10.

Figure 3.5 Insertion of angled dowel

Once the specimens were reinforced, they were stored under constant relative humidity and temperature for more than seven days. After that, the samples were

removed from storage, the provisional metallic straps were removed, and the samples were ready to test.

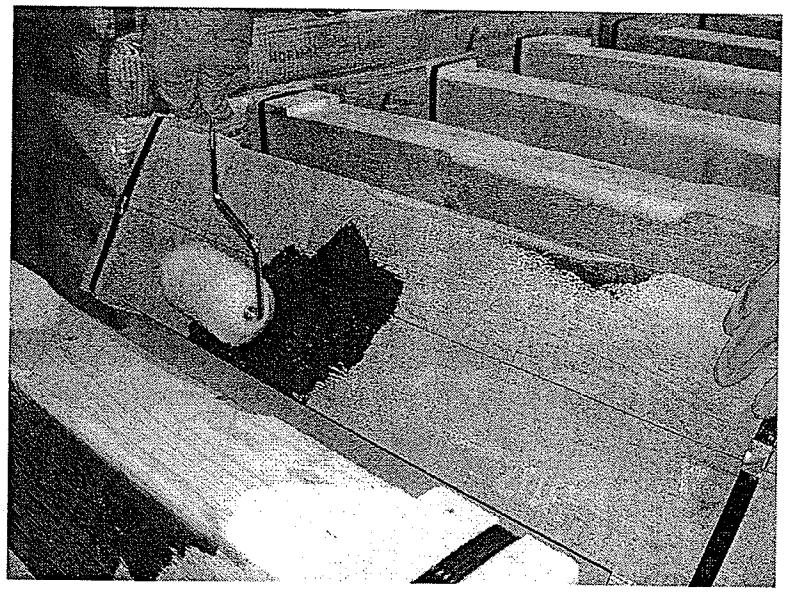

Figure 3.6 Application of saturant

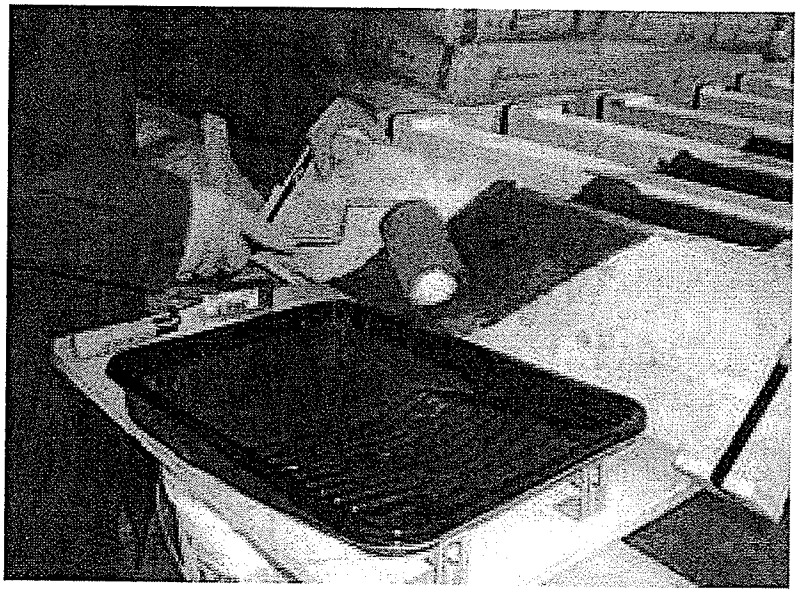

Figure 3.7 Application of first layer of epoxy resin

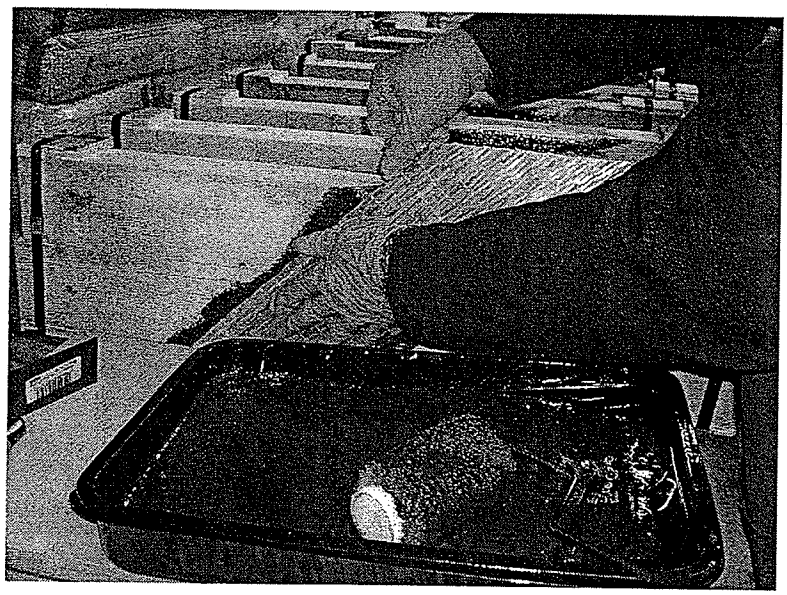

Figure 3.8 Setting dry FRP sheet into wet saturant

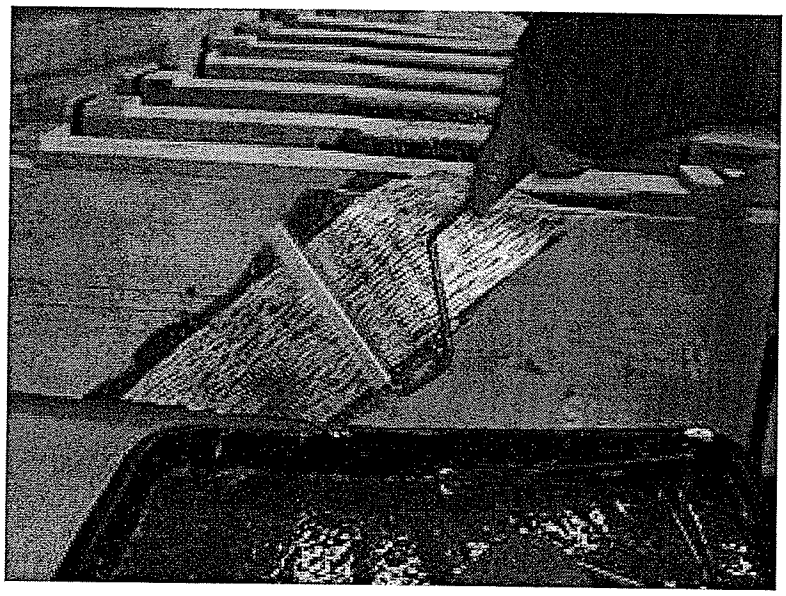

Figure 3.9 Pressing the FRP sheet using a roller

Timber is an anisotropic material that has the natural tendency to shrink and warp if cut and exposed to air. For this reason, even though they were kept at constant

humidity and temperature and regardless of strapping each specimen together, most of the pieces developed deformation after some time and a small separation between the two parts of the samples was observed.

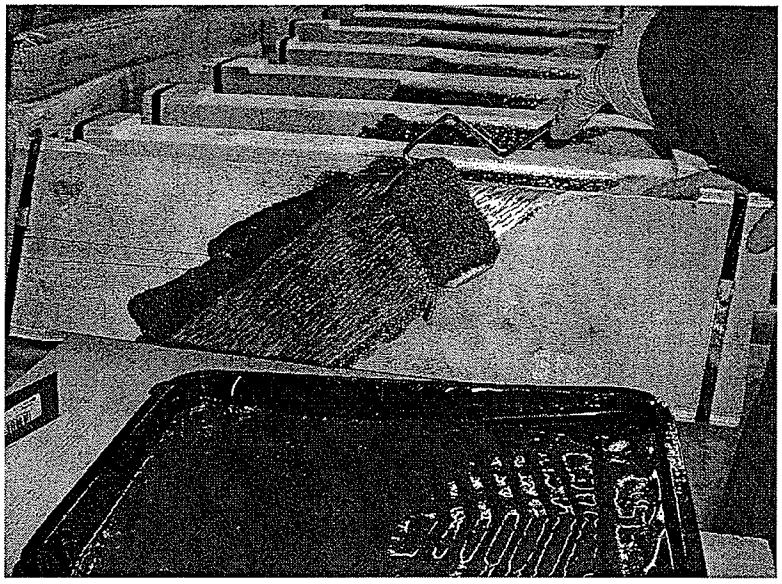

Figure 3.10 Application of top layer of epoxy resin

3.3.3 Test setup

A 250 kN testing machine was used to apply the load to the samples. This machine uses a manually controlled rate of loading and a vertical application of the load. The samples were set parallel to the loading head of the machine. A special set-up was designed using a frame to guarantee perfect alignment of the samples. The testing frame was formed by two towers of C steel sections attached to a plane surface and with lateral bracing on each side to avoid losing the alignment during the test as shown in Figure 3.11.

The samples were set in the frame using two steel blocks. One of the blocks was set as support on one side of the sample while the other was attached to the loading head of the machine. The two blocks were proportioned so they fit exactly into the grooves cut into the samples to obtain a direct shear load along the artificial split in the middle of each sample. This frame was designed specifically for this project. Design drawings are attached in Appendix A.

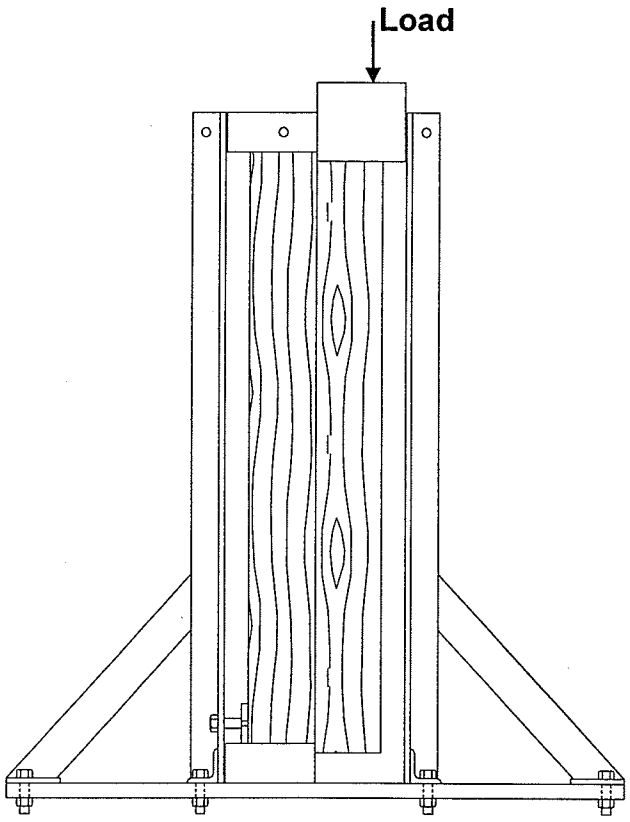

Figure 3.11 Shear frame with sample

Static load was applied at a rate of loading to produce failure of the specimens within 5 to 10 minutes. The test was a destructive test; load was applied to the samples till complete failure was observed. Continuous readings of the test

parameters were recorded using a DAQ system. Test setup is shown in Figure 3.12.

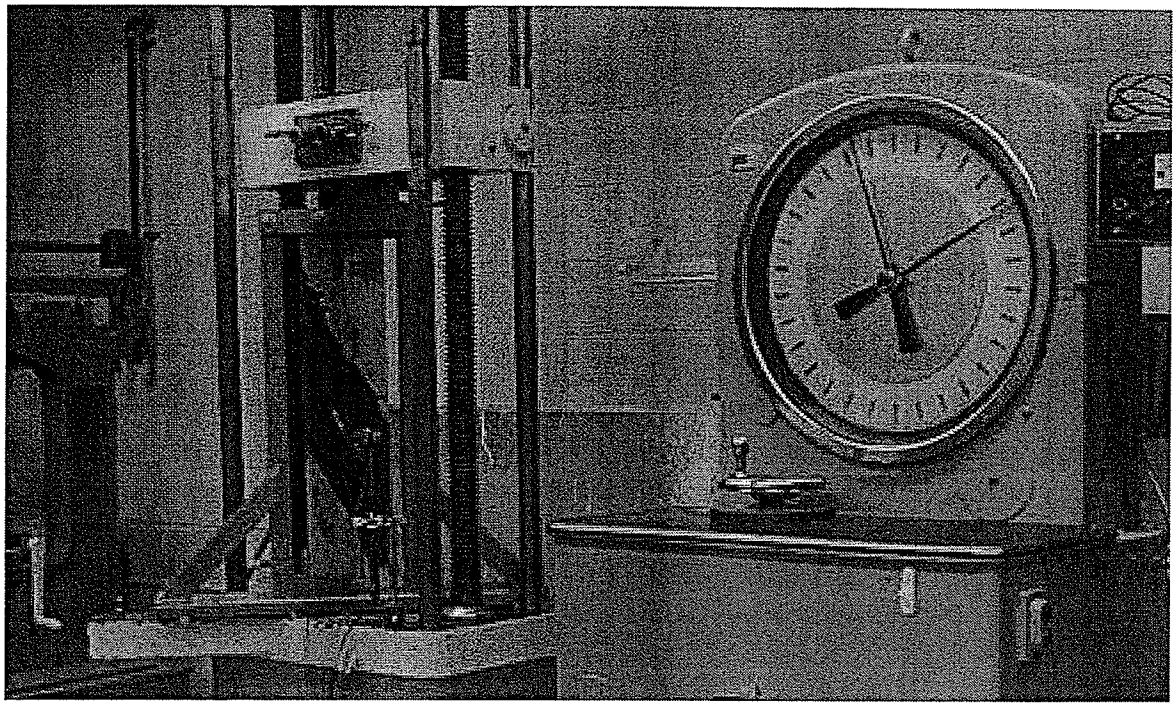

Figure 3.12 Shear test setup

3.3.4 Instrumentation

Each specimen was instrumented using PI gauges to measure strain in the direction of the reinforcement at each side of the specimen. Deformation of the sample was measured using linear variable displacement transducers – LVDTs – placed close to the centre of the specimen. LVDTs measured the total displacement in the direction of load. The test instrumentation is shown in Figure 3.13.

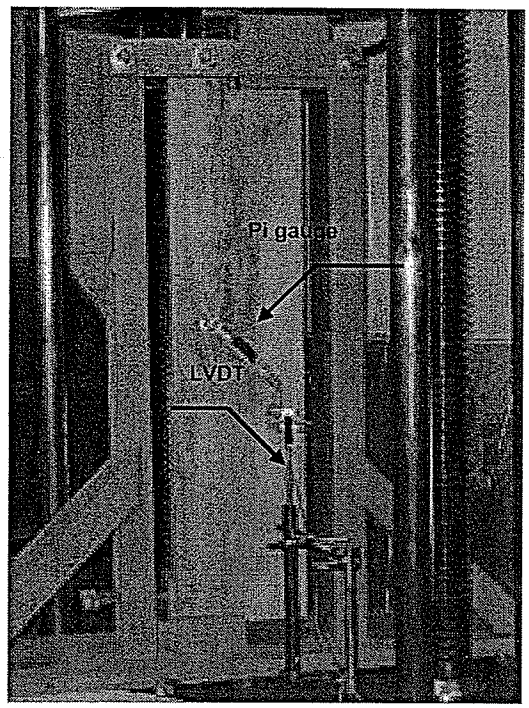

Figure 3.13 Shear test instrumentation

3.4 BENDING TEST

The purpose of this test was to evaluate the performance of old full-scale timber bridges retrofitted using GFRP sheets as shear and bending reinforcement. The test was prepared using the guidelines of ASTM standard D198 (ASTM 1999). The samples were tested in 3-point bending with load at midspan. The span for testing was 3.4 m except for beams Y1-206 and Y1-207 that were tested for a span of 3.28 m. The beams were tested before and after strengthening to compare the effect of the reinforcement pattern on the stiffness of the beams.

3.4.1 Test specimens

The timber beams used for this test were 9 sawn dimension timber beams, 100 mm x 400 mm x 3650 mm. The beams were taken from dismantled timber bridge and had dapped ends. They were visually graded according to the recommendations of the National Lumber Grades Authority (2002). Grading rules are used to determine the quality of commercial timber. The grade of an element is determined by visual inspection of size and position of the different characteristics of growth such as knots, checks, holes, pockets, rate of growth, torn, slope of grain, wane, knots and splits.

The timber beams used for this test were 40-years old, Douglas fir creosote-treated, and they were originally graded as select structural. As a result of aging, the beams had developed checks and splits that lowered their grade. The stringers were re-graded under the category "beams and stringers". According to the grading rule, beams and stringers with splits going through the entire cross section and longer than half of their depth (200 mm) should be downgraded to No.1. If the splits exceed 2 times the depth of the element (400 mm), the beam is downgraded to No.2. Finally, for splits longer than twice the depth of the element (800 mm) or 1/6 of its length (608 mm), the beam is considered grade reject and should not be used for structural applications.

The samples were also weighted and their moisture content was measured using a moisture meter, obtaining values ranging from 14.2 to 24.4%. A summary of the beam characteristics can be seen in Table 3.3.

Table 3.3 Summary of samples for bending test

Sample	Grade	Split length [mm]	Weight [kg]	Moisture Content [%]
Y2-201	1°	*	82.75	23.4
Y2-202	1°	*	93.55	24.4
Y2-203	Select Structural	*	97.85	21.4
Y2-204	2°	600	99.25	21.7
Y2-205	Select Structural	*	92.65	17.2
Y2-206	Reject	1540	85.65	21.4
Y2-207	Reject	880	85.06	20.2
Y1-208	Reject	2000	83.75	19.1
Y2-209	Reject	1200	85.05	14.2

* no split, only checks

The test samples were reinforced for flexure and shear. Flexural strengthening consisted of two layers of GPRP sheets on the tension face of the stringer along all their length and width. Shear strengthening was provided by GFRP straps 300 mm wide inclined 45° from the longitudinal direction. The straps were located at ends of the beams and wrapped underneath to guarantee development length and to prevent dap failures. The reinforcement layout is shown in Figure 3.14.

3.4.2 Strengthening procedure

Prior to strengthening, the splits were closed by drilling through the depth of the element and installing a ½" diameter bolt. All bolts were removed after the strengthening system was cured. Timber surfaces were prepared for application of sheets by cleaning the accumulated dust and other materials using a brush and vacuuming. The edges of the beams were rounded at locations where shear strengthening sheets should wrap around the wood; this is necessary to allow contact between timber and reinforcement and to avoid sharp transitions in the direction of reinforcement.

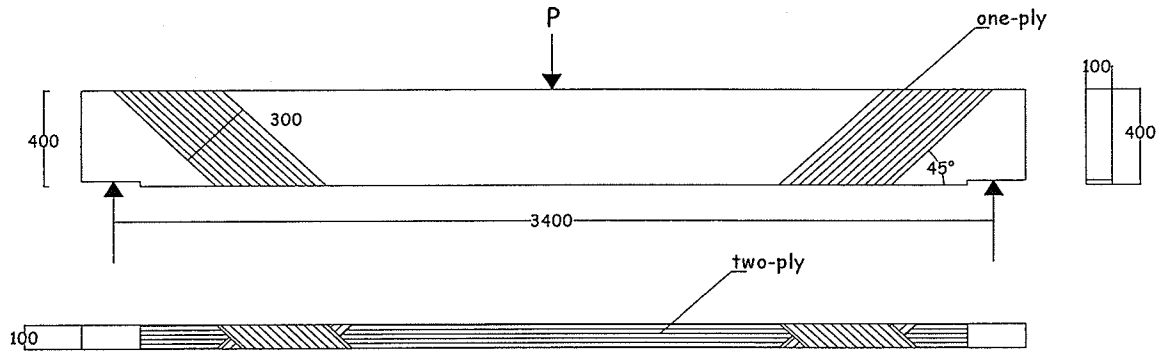

Figure 3.14 Reinforcing layout for bending test

The strengthening process is explained in Section 3.3.2. After the surfaces were cleaned and edges rounded, primer was applied followed by the first layer of saturant, reinforcing sheets were set and pressed against the surface, and a top layer of epoxy resin was applied. The same procedure was repeated according to

the layers of reinforcement and the process was finished with a layer of epoxy resin. Some images of the reinforcement process on the full-scale beams are shown in Figures 3.15 and 3.16. The sample beams were stored in the laboratory under constant temperature and relative humidity for curing for at least seven days before testing.

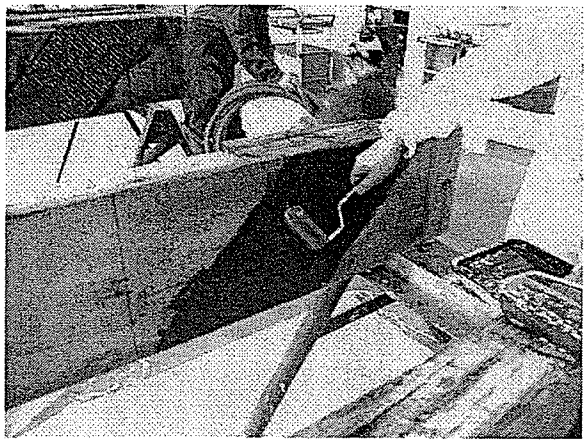

Figure 3.15 Application of first layer of epoxy resin on full-scale beams

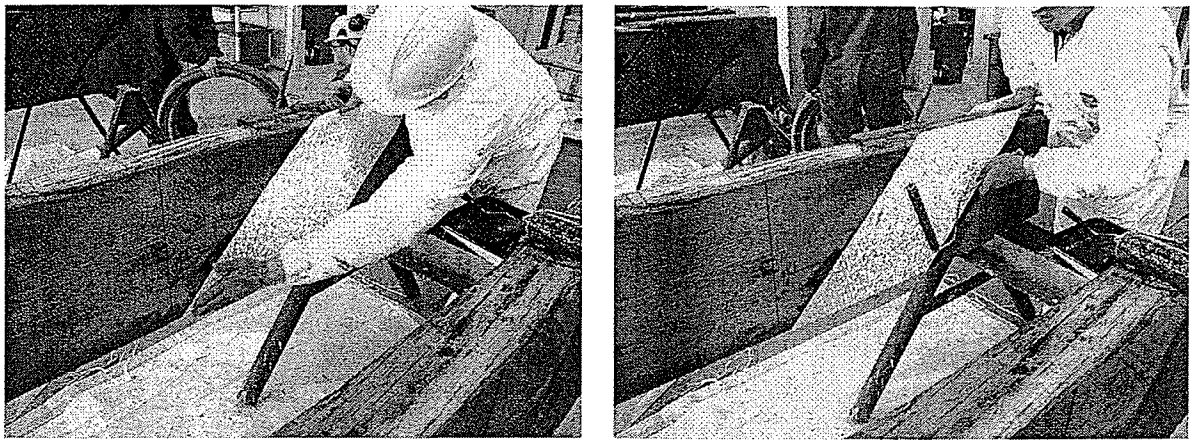

Figure 3.16 Application of GFRP reinforcing sheet on full-scale beams

3.4.3 Test setup

The beams were tested in 3-point bending under monotonic load using a stroke-controlled rate of load of 3 mm/minute to achieve maximum load within 6 to 20 minutes. The span was 3.4 m and the point of load was at midspan. Two tests were performed on each of the samples. The first test was a nondestructive test for measuring deflection of the beams prior to strengthening. In the second test, the beams were loaded up to failure.

The beams were supported on metal bearing plates over rollers to allow free rotation at the end of the specimens. The bearing plates were 200 mm long and extended across the entire width of the beams. The load was applied by a 1000 kN servo hydraulic machine. A 518 mm plate was used at point of application of the load to distribute the load and avoid local compression failure of the timber. Lateral supports were provided at the place of the bearing supports to restrict lateral deflection without producing any frictional restraint. Plaster bags were used at supports and at point of application of the load to level the samples and allow uniform distribution of the load. The test setup is shown in Figure 3.17.

3.4.4 Instrumentation

For the first test, the samples were instrumented with two dial gauges at midspan to measure displacement at the bottom of the beams. During the second test, each sample was instrumented with 6 mm strain gauges, 100 mm Pi gauges, and

200 mm Pi gauges. Strains in shear reinforcement were measured with two strain gauges on each end; the strain gauges were glued to the surface of the reinforcement at locations close to the beam splits or at midheight in the beams without splits. Strains on flexural reinforcement were measured with three strain gauges: one at midspan and one close to each support. Another measurement of strain in the shear reinforcement was taken with 100 mm Pi gauges on the opposite side of the strain gauges. Additionally, 200 mm Pi gauges were used to measure deformations at different heights of midspan. A total of six LVDTs measured deflection at the top of the beams in three different locations along the length of each side. A complete layout of the instrumentation can be seen in Figure 3.18. Data from the loading machine and instrumentation was recorded continuously with a data acquisition system.

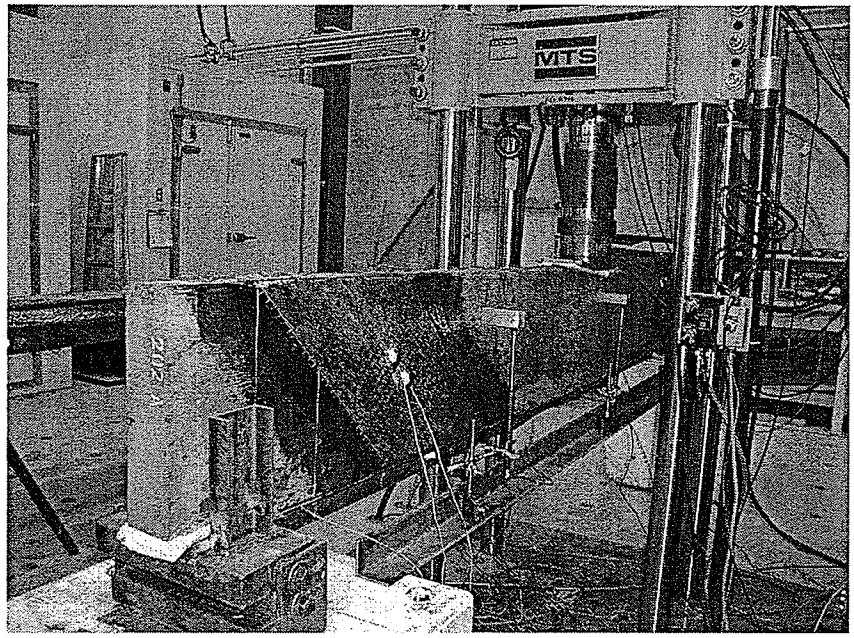

Figure 3.17 Test setup for bending test

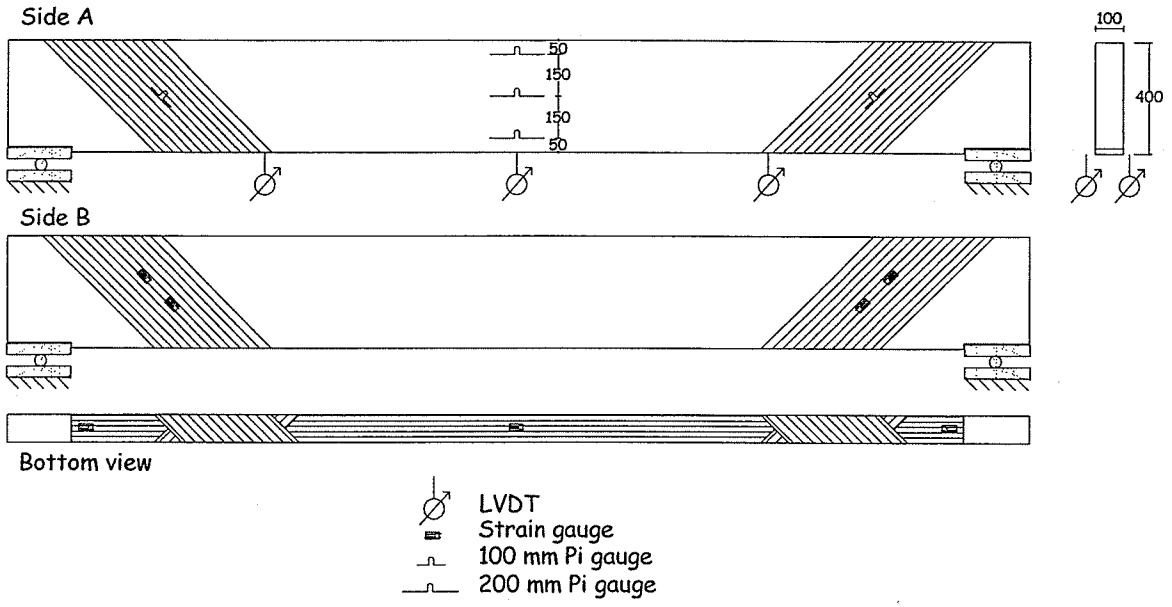

Figure 3.18 Instrumentation of bending test

3.5 DURABILITY TEST

This test was designed with the purpose of making an initial assessment of the durability of the proposed reinforcement system using GFRP sheets externally bonded to the surface of creosote treated timber beams. Eight full-scale beams already used for previous destructive tests were carefully inspected and subjected to cycles of changing temperature and relative humidity. The test was completed using a walk-in environmental chamber in the MacQuade Structures Laboratory. The samples were inspected at the end of monthly sets of cycles to determine visual evidence of new or additional debonding of the external reinforcement that could be produced by the exposure to the changing temperature and relative humidity.

Different standards to tests wood adhesives are available. However many of these existing standards use small samples and none of them were suitable for the purpose and size of the specimens employed in this experiment. Therefore the test was designed using guidance from previous research by Raknes (1997), who subjected full-scale samples to different environmental conditions and compared them with accelerated cycles produced in the laboratory.

3.5.1 Test specimens

Eight samples 100 mm x 400 mm x 3600 mm were reinforced using external GFRP fabric sheets for this test. All beams had been previously tested until failure in previous experimental programs, so some of them presented partial debonding of the reinforcement. The timber was creosote treated and the beams were reinforced using GFRP sheets glued to its surface using the same methods as described in section 3.4.2. Four samples were taken from the bending test that was part of this experimental program; the other four beam samples were taken from a previous test by Hay (2004). These beams had the same reinforcement pattern for shear without the bending reinforcement.

The samples were inspected and measured to determine the proportion of initial debonding due to their previous test and were then placed in the weathering chamber.

3.5.2 Weathering cycles

Controlled cycles of ranging temperature and relative humidity were achieved by introducing the test specimens into an environmental chamber with a controlled environment. The environmental chamber has exterior dimensions of 2.4 m x 6 m and 2.6 m height; with a temperature range from -40 to 40°C and humidity control range up to 90%. It is constructed with five inch thick woodless insulated panels. The air in the room is re-cycled continuously by a conditioning unit suspended from the ceiling with a system of fans, heaters and valves to meet the specified parameters. The controls of the chamber are attained with a graphical interface and expanded storage of data is recorded using a floppy disc.

The beams were arranged in the chamber with a spacing of 200 mm. The test extended during four months. Each set of cycles was completed within a month with weekly changes of temperature ranging from 20°C to 40 °C and relative humidity ranging from 25 to 85%. A summary of the cycling can be seen in Table 3.4.

Table 3.4 Cycling for weather test

	CYCLE	RH %	T° °C
Week 1	1	85	20
Week 2	2	60	40
Week 3	3	85	20
Week 4	4	25	25

Measurements of additional debonding of reinforcement were taken by visual inspection of the beams at the end of each monthly set of cycles. Some of the sheets were already debonded as a consequence of their previous test; extension of the damage was carefully measured and compared throughout the duration of the experiment.

CHAPTER 4

EXPERIMENTAL RESULTS AND DISCUSSION

In the first part of this section, results from the shear test are presented, making comparisons between the different shear patterns used in terms of shear capacity, modes of failure, rigidity, and stresses in the reinforcement. In the second part, results of the bending test are reported. The full-scale beams were reinforced for flexure and additionally for shear using a reinforcement pattern determined by the shear test. The different aspects presented are load-deflection behaviour, strain and stress in the reinforcement, failure modes, moisture content, and specific weight. In the third part of this section, results from the durability test are reported.

4.1 SHEAR TEST

4.1.1. Shear capacity

A wide range of load capacity was found for the different configurations of reinforcement tested as shown in Table 4.1. In general, the external reinforcement patterns exhibited larger load capacities than the bar reinforcing patterns and the smaller angles of reinforcement had larger capacities than the larger angles. External reinforcement patterns exhibited 77% to 100% higher

mean capacity to resist horizontal shear compared with bar reinforcement patterns.

After comparing different reinforcing patterns with the same reinforcement ratio, sheet reinforcement configurations showed larger mean values than their bar configuration counterparts. During the analysis of these results it is very important to take into account that the material used was the same as that of the actual full scale beams. The only difference is that the wood was not creosote treated.

Observation from previous investigations shows that creosote treatment has a significant impact on the bond properties between the timber surface and the FRP reinforcement. For this reason, the results from this test should be considered non conservative for the resistance of the external reinforcement on creosote treated timber.

A summary of results of the shear test is shown in Table 4.1. With increasing load, the bars or sheets became more parallel to the load, and the axial component of the force taken by them was larger making the reinforcement work more effectively. There was a transverse component of the resistance in the reinforcement, but it can be concluded that its effect was much less important than the axial component. In the case of the bars this can be seen clearly in the 90° angle configuration where the resistance is provided by transverse action only. In this configuration, all the force was transmitted by dowel action of the reinforcement. Regardless of the fact that this pattern used two bars instead of

one like the other cases, it was the worst configuration in terms of load capacity. Compared with the other configurations with the same reinforcement ratio of 0.3%, 1 ply at 30° and 1 bar at 30°, the two bars at 90° configuration obtained a mean value of only 28.25 kN compared with values of 80.1 kN and 40 kN for sheets and bar configurations respectively.

Table 4.1 Summary of shear test results

Configuration	Sample	ρ %	Pmax [kN]	Strain at Pmax [%]	Deformation [mm]
SHEETS:					
1 ply 30°	309	0.3	86	0.93	6.57
	310		70	0.4	2.82
	311		79	1.5	5.76
	312		88	0.65	2.78
	Mean=		**80.75**	**0.87**	**4.48**
1 ply 45°	305	0.21	47	0.26	1.57
	306		59	1.19	6.12
	307		57	0.75	0.91
	308		68	0.54	2.57
	Mean=		**57.75**	**0.68**	**2.79**
BARS:					
2 bars 90°	301	0.3	27	11.11	15.8
	302		32	8.65	18.5
	303		27	10.76	15.75
	304		27	8.39	19.48
	Mean=		**28.25**	**9.73**	**17.38**
1 bar 45°	313	0.21	29	1.77	3.65
	314		35	2.66	5.16
	315		33	2.52	6.16
	316		33	2.05	3.92
	Mean=		**32.5**	**2.25**	**4.7**
1 bar 30°	320	0.3	43	3.35	5.1
	319		40	1.85	4.16
	317		37	2.3	3.9
	Mean=		**40**	**2.5**	**4.38**

In the group of samples with reinforcement ratio of 0.21%, the 45° externally reinforced samples exhibited a higher capacity with a value of 57.75 kN and the samples that exhibited the smallest capacity were the ones reinforced with bar at 45° with capacity of 32.5 kN.

4.1.2. Failure modes

For the samples reinforced using GFRP bars, the entire 30° dowel samples failed in shear at average load of 40 kN. Failure was sudden and negligible deformation was measured by the LVDT at failure. The strains recorded by the PI gauges were small at failure compared to the other dowel samples, but were significantly larger than those measured on the sheet specimens. There was little evidence of any local compressive failure around the dowels, with the exception of one sample where localized wood failure was slightly noticeable. After failure, there were strands of FRP still intact, which contributed to large deflections and some resistance to load after peak load. This resulted in the dowels displaying a ductile mode of failure compared to the sheets, which failed suddenly with no noticeable deformation of the sheets.

All of the 45° dowel samples also failed in shear. Failure was sudden for all four samples. The deformations measured by the LVDT were greater than the deformations for the 30° samples, and so were the recorded strains in the direction of the dowels. Localized compressive failure of the wood around the

dowels was noticeable in these samples, which may have attributed to the larger deformations and strains.

All four of the 90° dowel samples experienced local compressive failure of wood under dowels followed by dowel pull-out and in two samples the eventual shear failure of the dowels. The deformations measured by the LVDT and the strains measured by the PI gauges were 5 times larger in comparison with the angled samples. These large deformations and strains can be attributed to the localized wood failure around the dowels as well as the pull-out of the dowels. The pull-out is a result of the wood/epoxy interface not providing enough bond strength.

FRP bar reinforced samples experienced large deformations before failure as shown in Figure 4.1. FRP bar failures were initiated by splitting of the bar that was no longer able to carry its full capacity; however some residual capacity was still available. Even after the bar had initially cracked longitudinally, some of the fibres were still carrying load. This mode of failure contributed to the bar configurations ductile failure and allowed the reinforced member to absorb a significant amount of energy before collapse.

The failure mode for all of the FRP sheet specimens was the debonding of the reinforcement. The sheets developed around 30 to 40% of their capacity and then failed suddenly. Some of the samples failed at the interface between the wood and the sheet with the tearing off of some fibres of wood (Figure 4.2), but most of them failed within the wood itself (Figure 4.3). When comparing this test

with results from previous investigations, it was observed that the debonding failures of the creosote treated timber beams were in the interface between the creosote and the reinforcement. This confirms that the results from this test are not conservative and that creosote plays an important role in the bond strength of the externally reinforced members. Further studies on creosote treated smaller samples should be carried out.

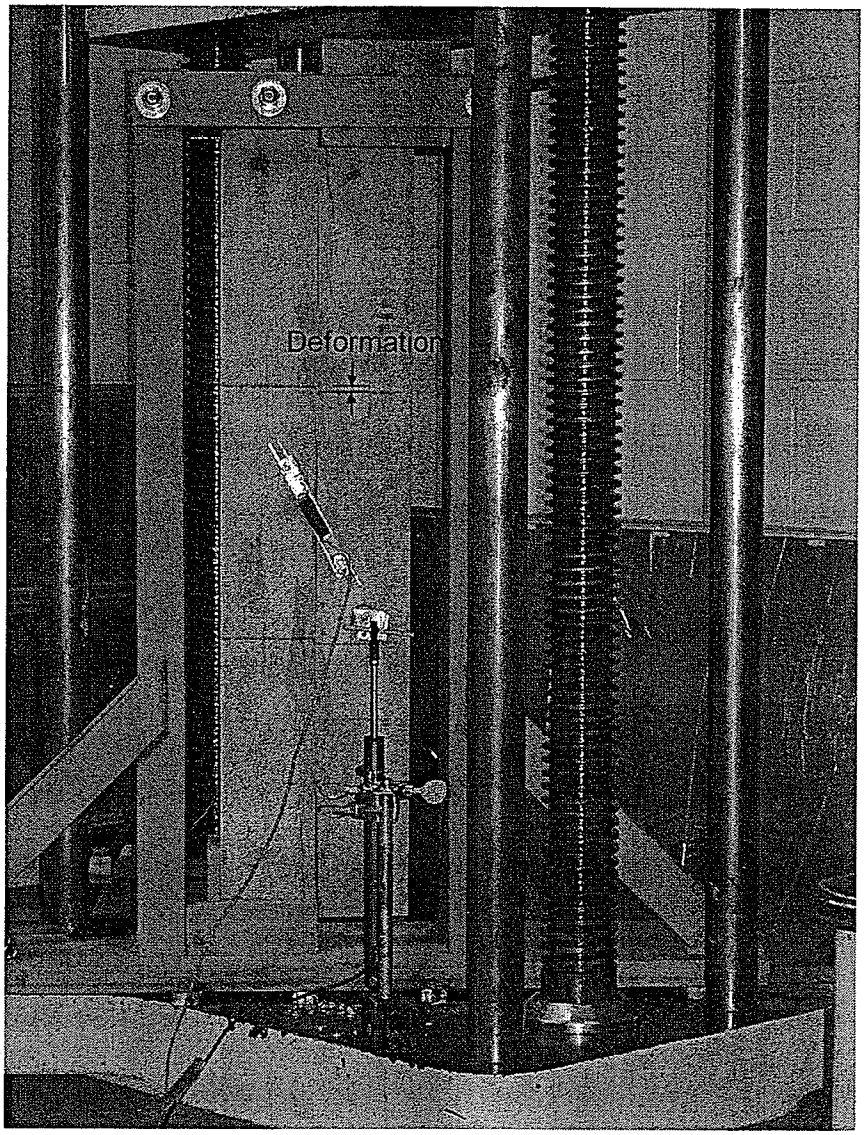

Figure 4.1 Shear test of 90° bar-reinforced sample

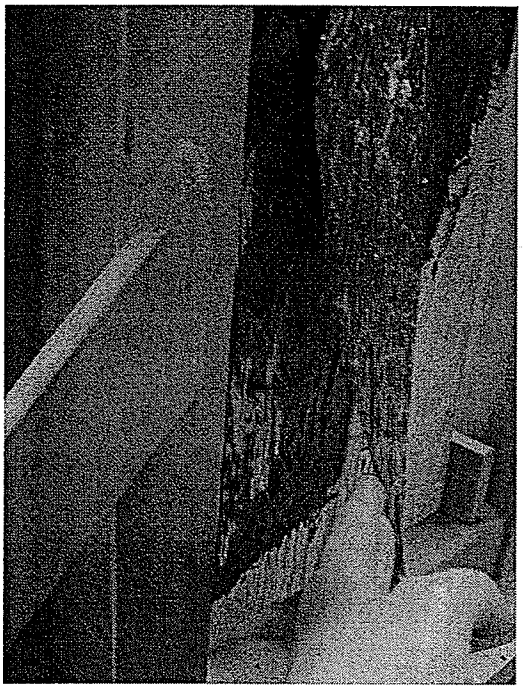

Figure 4.2 Debonding failure at the interface between the wood and the sheet.

Figure 4.3 Debonding failure with tearing of wood fibres

For the 45° configuration of the sheet samples, strains in the reinforcement at ultimate varied from 0.26% to 1.19%. This was a large range of variation considering that the maximum strain was more than three times the smaller strain. The mean value of strain at ultimate for this configuration was 0.68%, while the maximum strain on the reinforcement according to the manufacturer is 2.1%. It was found that for this configuration, the sheets are developing a mean value of 32% of their capacity.

For the 30° scheme, the strain at ultimate ranged from 0.4% to 1.5%. This corresponds to a mean value of 41% of the capacity developed by the sheets. Comparing the mean values, a 9% increase in the capacity of the sheet was obtained. An explanation of this behaviour is that the 30° configuration allows for a larger size of sheets, and larger development length available. For these unidirectional sheets the fibres were closer to the direction of the force compared to other angle orientations. This confirms that the capacity of the reinforced member to resist shear can be increased by increasing the development length of the sheets and effectively utilizing fibre direction. If length is not available on stringers, anchorage should be provided by at least one longitudinal sheet applied horizontally on the free end of the shear reinforcement.

4.1.3. Rigidity

A wide range of values of final displacement were obtained from the set of reinforcing patterns. The values of load were plotted against longitudinal

displacement. The plots can be seen in Figures 4.4 to 4.8. The initial slope of the curve for each specimen is an indicator of the rigidity of the configuration.

Table 4.2 Rigidity of specimens in the shear test

Sample	Configuration	ρ %	Pmax [kN]	Displacement at 10 kN [mm]	Load / Displacement [kN/m]
SHEETS:					
309	1 ply 30°	0.3	86	0.0213	0.469
310			70	0.0267	0.375
311			79	0.0186	0.538
312			88	0.0115	0.870
Mean=			**80.75**	**0.020**	**0.512**
305	1 ply 45°	0.21	47	0.0354	0.282
306			59	0.0297	0.337
307			57	0.0512	0.195
308			68	0.00717*	1.395*
Mean=			**57.75**	**0.039**	**0.258**
BARS:					
301	2 bars 90°	0.3	27	0.412	0.024
302			32	0.594	0.017
303			27	0.483	0.021
304			27	0.535	0.019
Mean=			**28.25**	**0.506**	**0.020**
313	1 bar 45°	0.21	29	0.383	0.026
314			35	0.308	0.032
315			33	0.446	0.022
316			33	0.383	0.026
Mean=			**32.5**	**0.380**	**0.026**
320	1 bar 30°	0.3	43	0.233	0.043
319			40	0.229	0.044
317			37	0.225	0.044
Mean=			**40**	**0.229**	**0.044**

*Atypical values were not taken into account in the calculation

The samples reinforced with bars showed low rigidity in comparison to the sheet reinforced samples as shown in Table 4.2. The 30° samples had the highest rigidity of the bar reinforced samples, significantly higher than the other two reinforcing schemes. The two dowels aligned at 90° had the lowest rigidity. It is clear that the angle of reinforcement has a significant effect on the rigidity of the specimen. The plots in Figures 4.4 to 4.6 show the high rigidity of the 30° samples compared to the 45° and 90° samples.

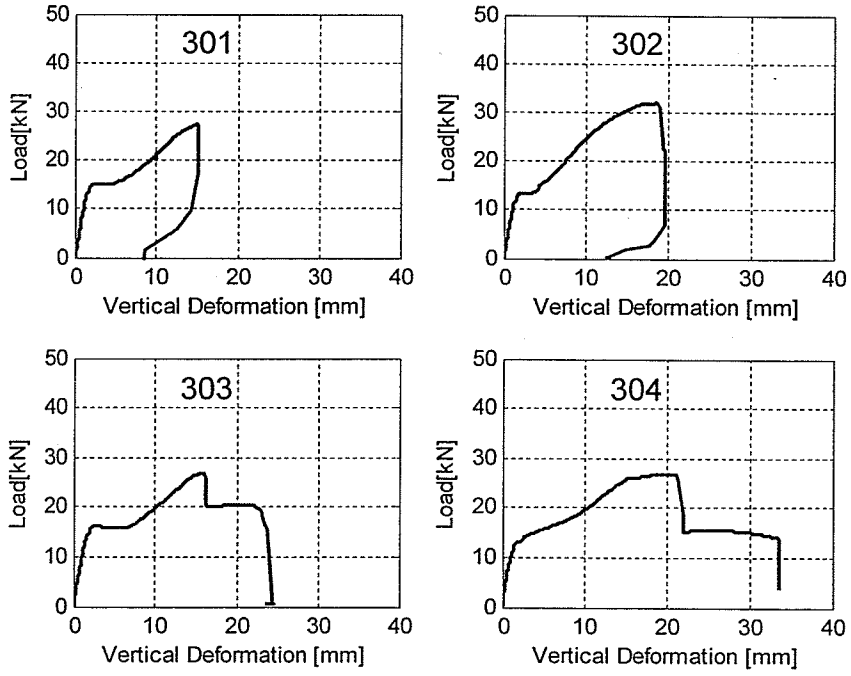

Figure 4.4 Behaviour of specimens reinforced by 2 bars at 90°

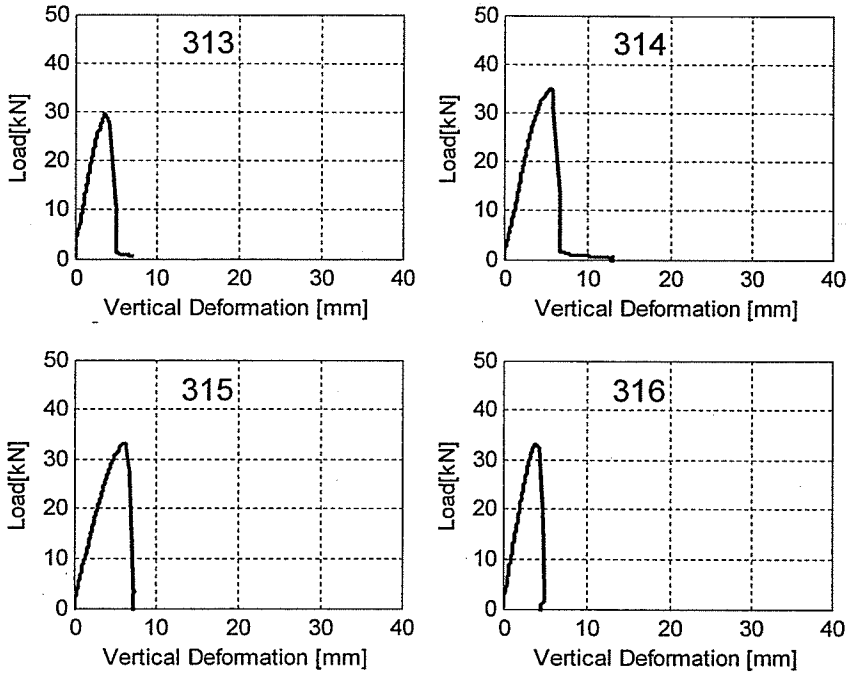

Figure 4.5 Behaviour of specimens reinforced by 1 bar at 45°

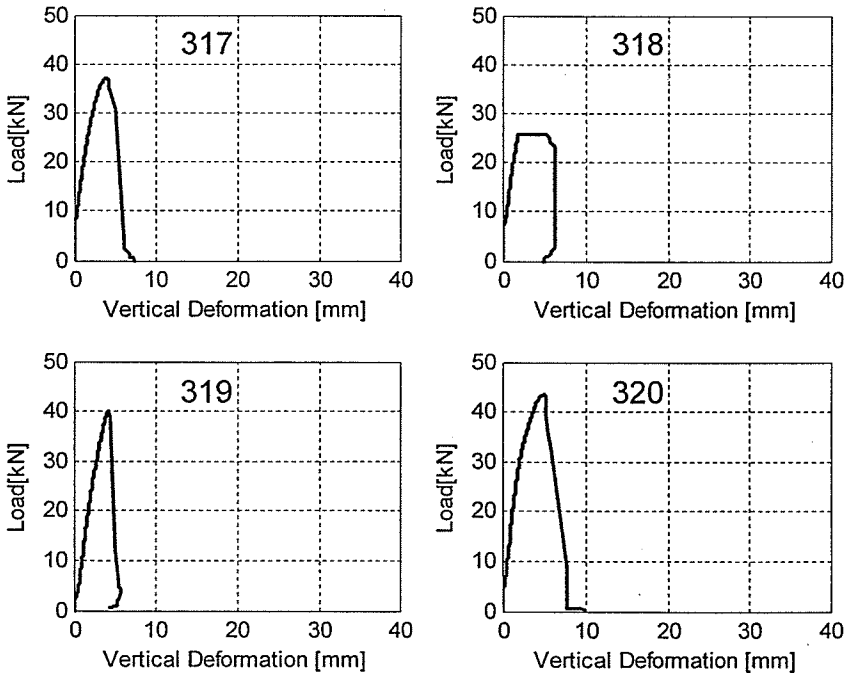

Figure 4.6 Behaviour of specimens reinforced by 1 bar at 30°

FRP sheet reinforced samples were about ten times more rigid than bar reinforced samples. There is a direct relationship between rigidity and the angle of the reinforcement. In terms of rigidity, the samples reinforced with an angle of 30° performed better than the samples reinforced with an angle of 45°. Figure 4.7 and 4.8 show plots of load against vertical deformation for both patterns. Negligible deformations were recorded for all samples. The mean value of the load/deformation ratio for the 30° configuration was almost twice the value of the 45° degree angle configuration.

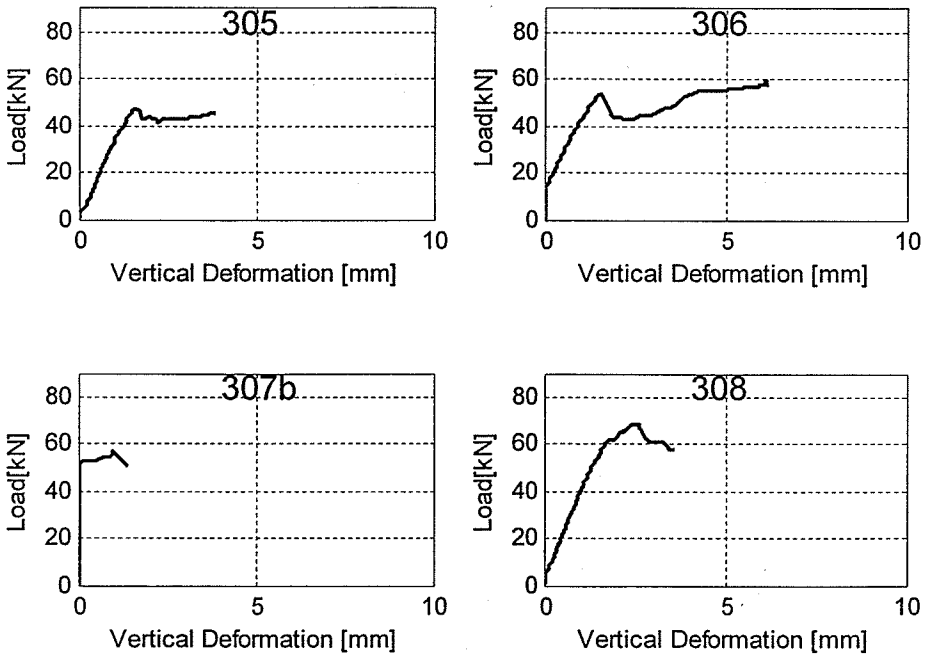

Figure 4.7 Behaviour of specimens reinforced by 1 ply at 45°

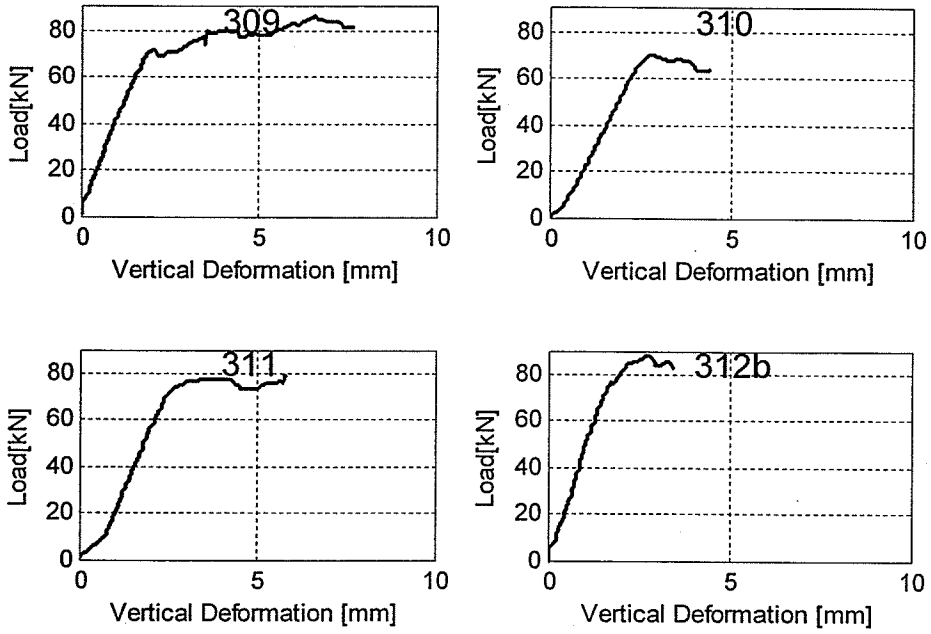

Figure 4.8 Behaviour of specimens reinforced by 1 ply at 30°

4.2 BENDING TEST

Results from this study have been combined with data from previous tests on samples of similar characteristics and dimensions. The complementary samples includes eight control stringers (Beams C) and six bar-reinforced stringers (Beams B) tested in 3-point bending with the load at midspan (Amy 2004), and 16 stringers reinforced with the same shear reinforcement and no bending reinforcement (Beams S). These stringers were tested in 3-point bending with load at quarter-span (Hay 2004). A summary of the test samples analyzed is shown in Table 4.3.

The aged beams used for this study had large splits along the grain that lowered their quality. Results from the bending test are presented according to the grade of the stringers to observe the effect of the reinforcement on the timber of varying quality.

Table 4.3 Dimension and characteristics of test samples

Beams	Width [mm]	Depth [mm]	Length [mm]	Reinforcement		Point load position
				Type	Configuration	
Beams C *	100	400	3650	none		midspan
Beams B *	100	400	3650	bars	shear and flexure	midspan
Beams S **	100	400	3650	sheets	shear only	quarterspan
Beams SF ***	100	400	3650	sheets	shear and flexure	midspan

* Amy and Svecova, 2004
** Hay, 2004
*** current study

4.2.1 Failure modes

Beams SF exhibited three failure modes: (1) compression perpendicular to grain, (2) flexure, and (3) shear failure by debonding of shear reinforcement. A summary of failure modes is shown in Table 4.4.

Beams Y2-202, Y2-203, Y2-205 and Y2-208 failed in compression perpendicular to grain, also called bearing failure, at the point of application of the load. Beams that exhibit this kind of failure were specimens without long splits. The exception was beam Y2-208, which had a 2000 mm split; however its position at 305 mm

from top of the beam was away from midheight, where critical shear forces are developed.

Table 4.4 Bending test results for Beams SF

Sample	Grade	Split			EI			P	Failure mode
		Length A	Length B	Distance from top	Before strength.	After strength.	Improv.	max	
		[mm]		[mm]	[N.mm^{2}x10^9]	[N.mm^{2}x10^9]	%	[kN]	
Y2-203	SS				4327	4830	11.6	157	Bearing
Y2-205	SS				4844	4929	1.8	151	Bearing
Y2-201	1°				3923	4012	2.3	127	Flexure
Y2-202	1°		320	210	4178	4454	6.6	120	Bearing
Y2-204	2°		600	205	4642	5650	21.7	132	Shear
Y1-206	Reject		1540	220	2246	3985	77.4	130	Shear
Y1-207	Reject	875	880	215*,180**	2636	3997	51.6	130	Shear (A)
Y2-208	Reject		2000	305	2546	3831	50.5	130	Bearing
Y2-209	Reject		1200	205	2695	4386	62.7	134	Shear

* End A
** End B

Bearing failure is considered a strong mode of failure that elements can reach when they are strong enough to resist stresses associated with shear and tension. Reinforced beams may reach this mode of failure because of the action of shear and flexural reinforcement that bridge the natural defects of the timber. Beams with this kind of failure supported loads ranging from 119.56 kN to 156.52 kN, corresponding to a mean stress of 2.69 MPa at the point of application of the load and 3.48 MPa at supports, according to the sizes of the bearing plates. The

design value for compression perpendicular to grain according to CSA 086.01 is 7.0 MPa. An explanation of the low failure stress could be the negative effect of the nails used to attach the laminated deck. All bearing failures occurred at the point of application of the load where nails were removed prior to the test to avoid concentration of stresses at the location of the nails. The large number of nails at the top face of the beams produces damage to the upper portion of the elements providing means for the moisture to penetrate the timber. The failure by compression perpendicular to grain can be seen in Figure 4.9.

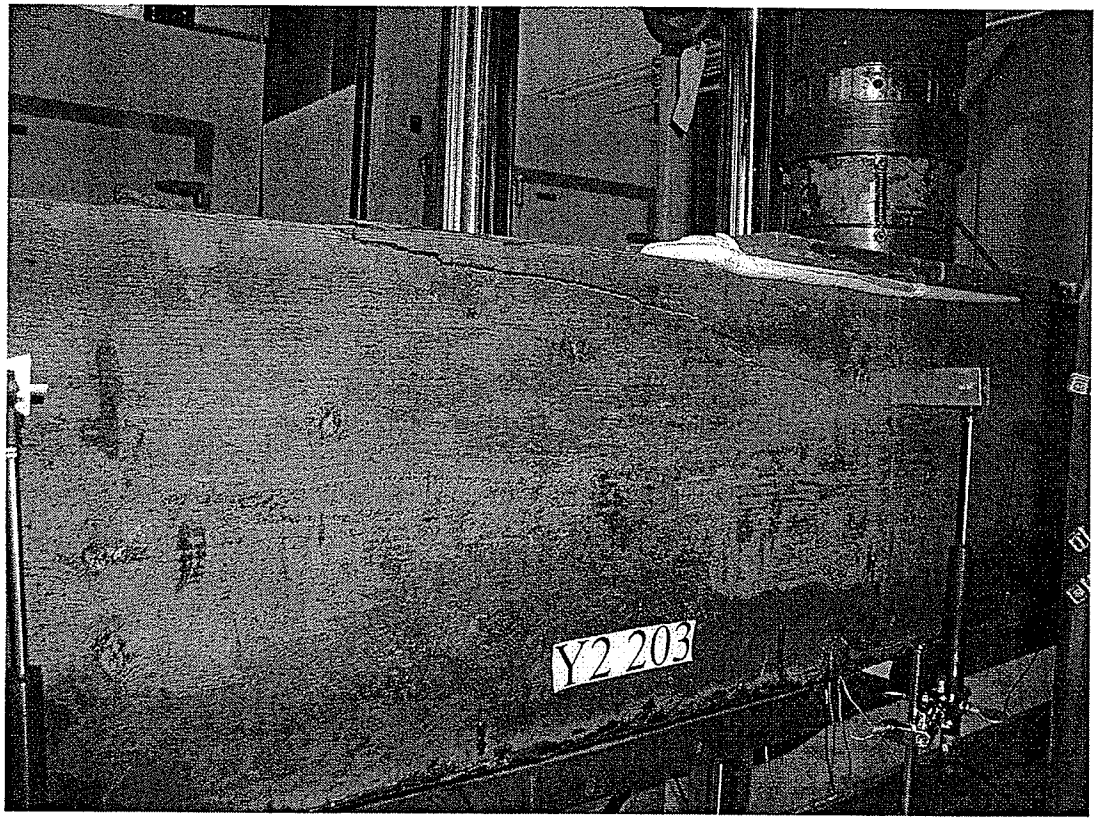

Figure 4.9 Failure by compression perpendicular to grain

One flexural failure was observed in specimen Y2-201 at a maximum load of 126.99 kN (Figure 4.10). This failure was characterized by longitudinal separation of fibres close to midspan and at a low height.

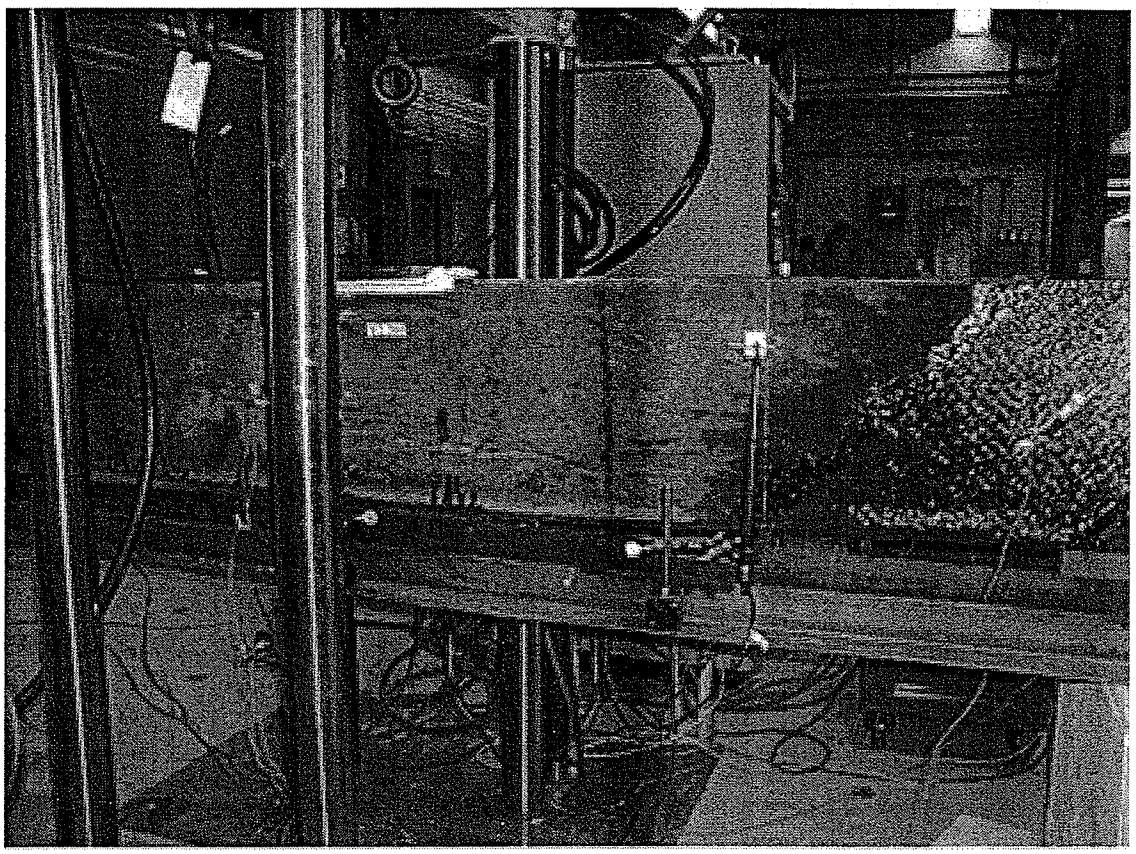

Figure 4.10 Flexural failure

Four shear failures were observed in beams Y2-204, Y1-206, Y1-207 and Y2-209. Shear failures were produced by debonding of the shear reinforcement at loads ranging from 129.75 kN to 134.07 kN. The mean shear strength of these stringers was 2.46 MPa, with a minimum value of 2.43 MPa. These values can be compared with results for Beams S with shear stress at ultimate load of 3.84 MPa in average and 2.5 MPa at the 5^{th} percentile level (Hay, 2004). For control specimens, Hay reported values of 2.9 MPa and 1.9 MPa in average and at 5^{th} percentile level, respectively. According to the previous values, the control specimens reported shear strength higher than the design value of 1.1 MPa as per CSA O86-01 (2001), or 0.9 MPa as per CHBDC (2000); shear capacity of the

reinforced beams from both test programs is higher compared to the two code values.

Most of the debonding failures were initiated at the interface between the timber and the sheets as shown in Figure 4.11. This behaviour indicates that the reinforcing system could be improved in order to increase the bonding resistance. Some of the debonding failures were initiated within the timber itself, as observed in Figure 4.12. These failures were accompanied by large slip deformations along the splits ranging from 4 to 8 mm (Figure 4.13).

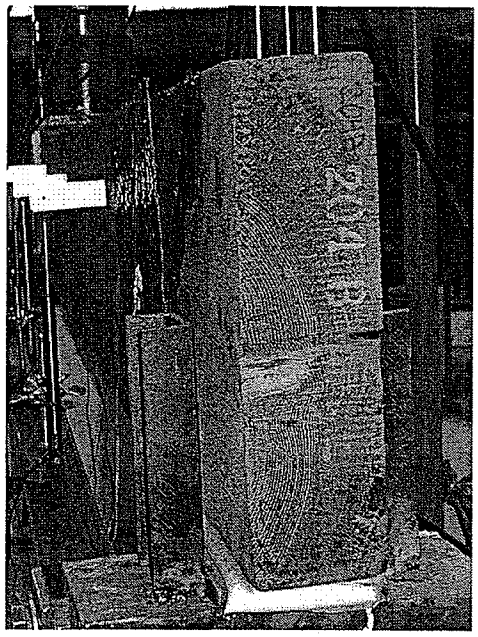

Figure 4.11 Debonding failure between the wood and the reinforcement

All beams that failed in shear were graded as Reject or No. 2, with splits longer than their depth (400 mm). Beam Y2-208 did not fail in shear although it had a long split as shown in Figure 4.13. In beam Y2-208, the split was at a low height; this shows that large splits are not critical for shear if they are not close to midheight, which is the location of maximum horizontal shear stresses.

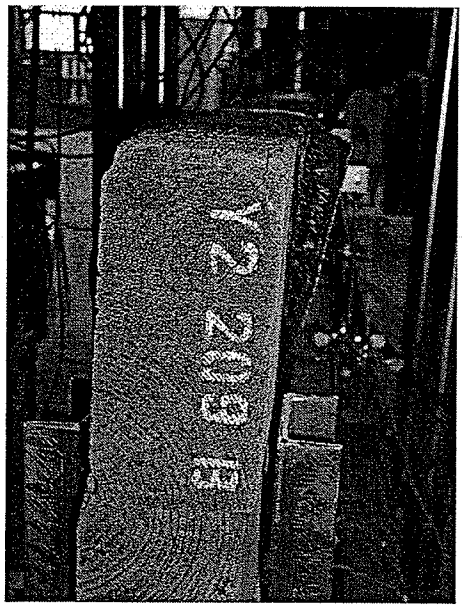

Figure 4.12 Debonding failure with tearing of wood fibres

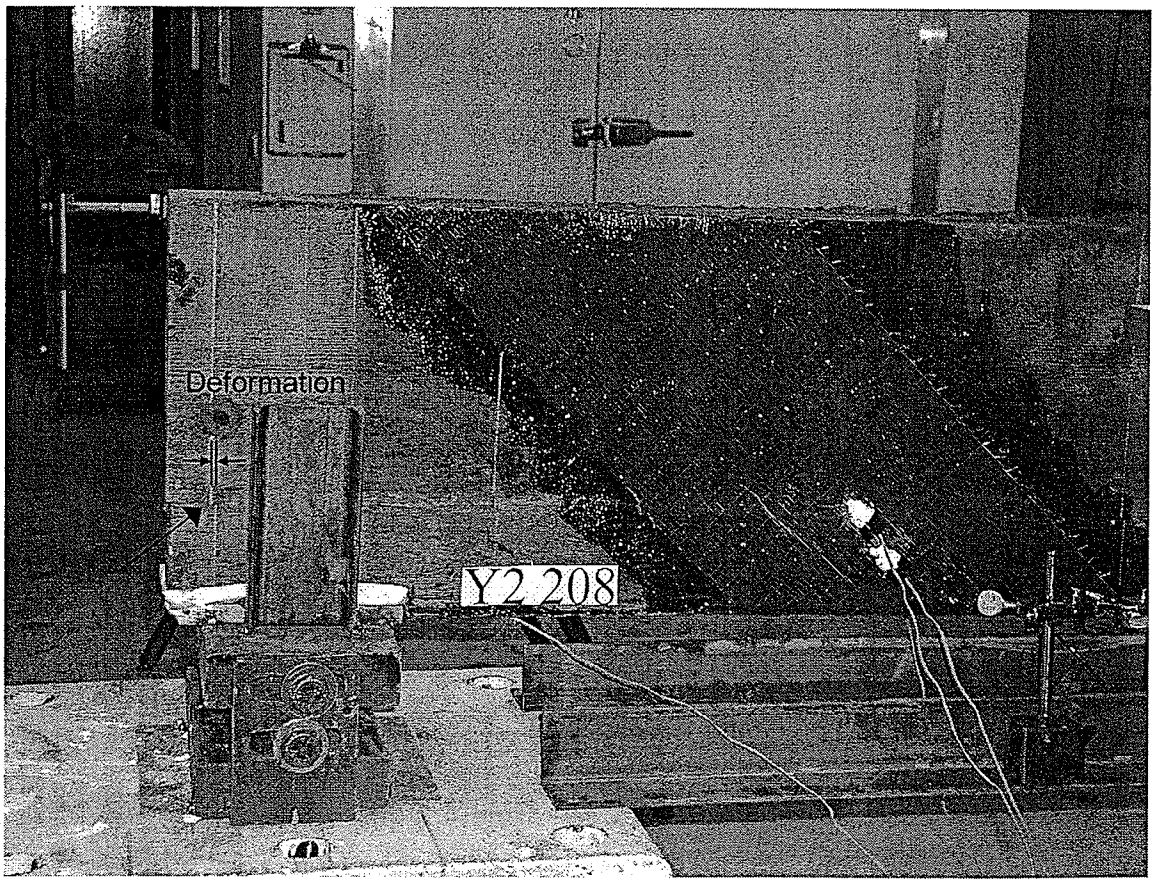

Figure 4.13 Slip deformation along split

4.2.2 Rigidity

Deflection measurements from the tests on beams before and after strengthening were compared to analyze the effect of reinforcement on the stiffness of the strengthened elements. Additionally, strength results from destructive test on strengthened elements were compared to strength results from the control beams and the beams reinforced for shear and flexure with GFRP bars.

Stiffness of the beams was calculated by plotting values of deflection against applied load and using deflection equation for 3-point bending at midspan:

$$\Delta = \frac{PL^3}{48EI} \tag{4.1}$$

In Equation 4.1, Δ is the deflection measured at midspan, P is the applied load, L is the span, E is the modulus of elasticity of timber, and I is the moment of inertia of the section.

Calculated values of stiffness EI are summarized in Table 4.4. Beams graded as select structural, No.1, and No. 2 had a mean stiffness equal to 4383 $x10^9$ $N.mm^2$ compared with a value of 2531 $x10^9$ $N.mm^2$ for reject grade beams. Lower grade beams are 42% less stiff than better quality beams. This behaviour is explained by split beams acting at the split ends as two with smaller moments of inertia.

Split beams exhibit a larger improvement in stiffness after strengthening compared with non-split beams because of the effect of shear reinforcement. The reinforcement ties split ends together increasing the moment of inertia of the section. Table 4.4 shows a mean stiffness improvement of 60.5% for grade reject beams compared with a mean value of 8.8% for No. 1, No.2, and select structural beams.

An analysis of variance between groups, ANOVA, was performed to evaluate if there was a significant difference between means of stiffness, EI for beams before and after strengthening. The ANOVA analysis was used to test the null hypothesis; if the test is significant, the null hypothesis can be rejected. The null hypothesis for this analysis was that the means of the two groups are equal; therefore there is no stiffness improvement.

ANOVA tests the null hypothesis by comparing two different estimates of variance, one based on variances within the samples and other based on variances of sample means. P-values obtained from ANOVA lower than 0.05 to 0.01 indicate that means of the groups being compared are significantly different and therefore the null hypothesis can be rejected. A p-value of 0.037 was obtained from the analysis on the two groups of beams. This result indicates that the mean stiffness of beams before and after strengthening are significantly different from the statistical point of view, therefore a real improvement in stiffness was obtained using the proposed strengthening scheme.

Further comparison considering beam grade revealed that mean values of EI of reject grade beams before strengthening are significantly different from mean values of reject grade beams after strengthening. A very small p-value of 6.78×10^{-6} indicates that differences are highly significant. Mean values of upper grade beams before and after strengthening however, are not significantly different. The effects of strengthening are beneficial primarily for increasing the stiffness of lower grade beams.

4.2.3 Load-deflection behaviour

Figure 4.14 shows the load-deflection graphs of the tested beams. In general, the graphs show similar behaviour for all the reinforced samples regardless of the lengths of splits. The superior capacity of the select structural beams can be observed from the graph, but it also shows that the strengthening process successfully improves the uniformity in the behaviour of the beams that were originally of various grades.

Beams of original high quality which had bearing failures, (Y2-203, Y2-205 and Y2-202) had load-deflection curve shapes characterized by a flat portion close to ultimate load. At failure, the beams continued deforming without an increase in the applied load as a result of the crushing of wood fibres at the loading point.

Split beams that failed by shear (Y2-204, Y1-206, Y1-207, and Y2-209), exhibited large deformations and a sudden drop in the load at ultimate when the

reinforcement debonded and shear failure occurred. Beam Y2-201, that failed in flexure, exhibited a sudden drop in load at ultimate; a lower load was sustained by the beam after this point. The beams that failed in shear did not have the ability to sustain load after the peak load.

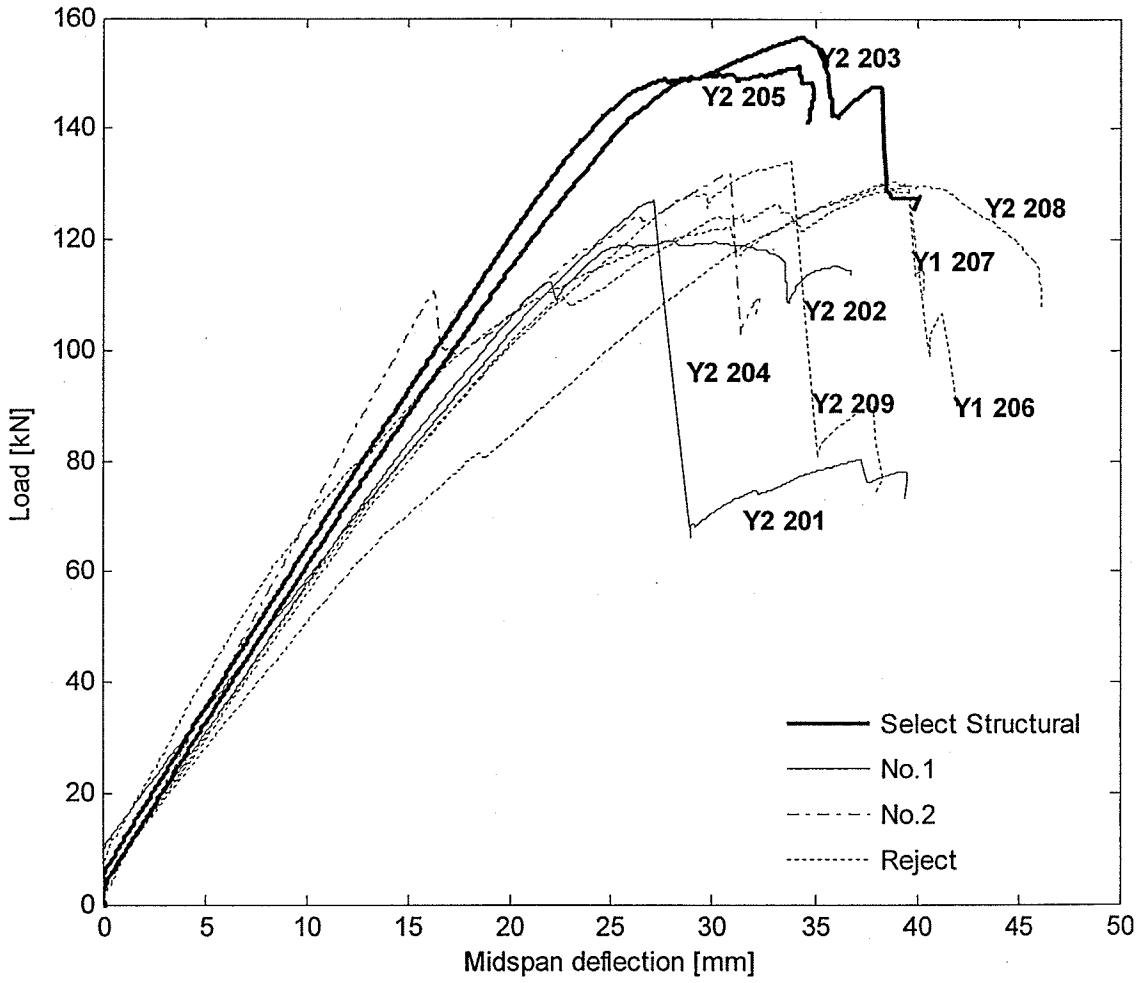

Figure 4.14 Load deflection curves

Load-deflection graphs show that all of the reinforced beams exhibited ductile behaviour with large deformations before failure. Some of the beams, Y2-208, Y2-204, and Y2-205, had a slight difference between the measurements of

deformation taken at each side of their section. This is due to a rotation of the beams at the support due to the warp of these beams as shown in Figure 4.15.

4.2.4 Strength

The effect of the type of reinforcement on strength improvement was investigated comparing the current test results with reported values of control and bar-reinforced beams tested by Amy (2004). These beams were reinforced with 2-#12 GFRP bars on the tension face corresponding to a reinforcement ratio of 0.75% and 3-#12 shear dowel bars at each end, inclined at 60° with the axis of the beam, corresponding to a reinforcement ratio of 0.28%. Control specimens were selected visually as beams with superior condition to beams that were reinforced. Amy reported mean values of 121.3 kN ultimate load with standard deviation of 22.6 kN for the control beams and 149.2 kN ultimate load with 25.5 kN standard deviation for the reinforced beams equivalent to an increase of 22% in ultimate load of reinforced beams over control beams. In comparison, for the nine full scale beams with external reinforcement tested in this research, values of ultimate load equal to 134.49 kN with a standard deviation of 11.75 kN were reported. It corresponds to an increase of 10.8% over control beams. A summary of these results is shown in Table 4.5.

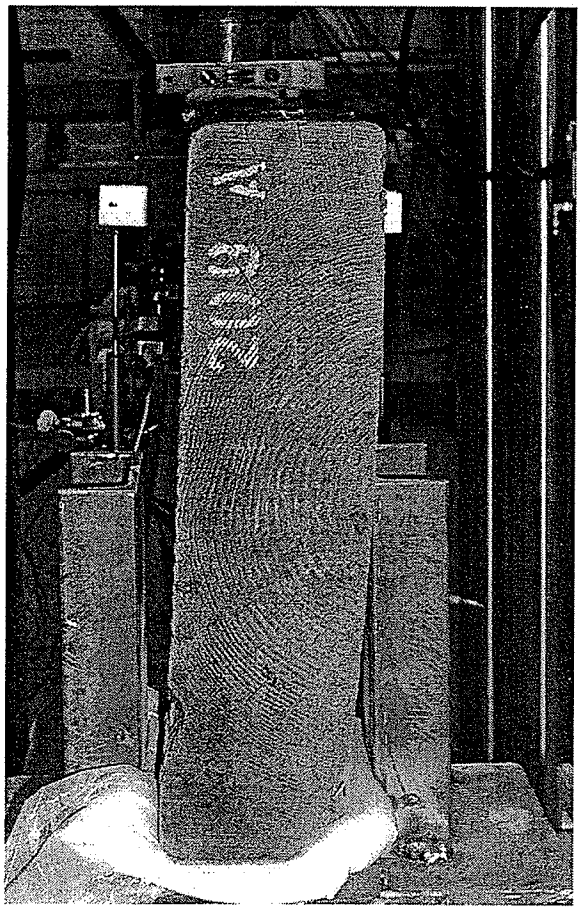

Figure 4.15 Turning of the beam over the support

Table 4.5 Mean maximum loads for flexure test

Beams	# of samples	Reinf. ratio Bending %	Reinf. ratio Shear %	P max. [kN]	Standard deviation [kN]	Improv. %
Beams C *	8	0	0	121.3	22.6	N/A
Beams B *	6	0.750	0.280	149.1	25.5	22.9
Beams SF	9	0.176	0.163	134.5	11.75	10.8

* Amy and Svecova, 2004

Beams reinforced with the proposed reinforcement pattern using GFRP sheets exhibited a significant improvement in strength with smaller amount of reinforcement. They also exhibited a reduction in variability between the control and bar reinforced beams. Limitation on the number of samples tested does not allow more conclusive analysis regarding variability.

4.2.5 Strains in shear reinforcement

Results from this experimental program were combined with values reported by Hay (2004). The beams used for comparison were reinforced with the same shear reinforcement pattern but without the flexural reinforcement and will be referred as Beams S. These beams were tested until failure in 3-point bending with the point load at quarter span. Each of the beams was tested twice, one test with the load close to each support. Table 4.6 contains values of strain on the shear reinforcement for the Beams SF tested at midspan. Table 4.7 and Table 4.8 contain values of strain for Beams S tested at quarter span. The tables show values of microstrain and maximum loads as well as split length and split depth. The values are reported for each side of the beams in Table 4.6 and for the sides failing in shear in Table 4.7 and Table 4.8. Split depth, kd, was measured from the top of the beams and it is also expressed as a fraction, k, of the depth of the beam, d.

For the Beams SF that did not fail in shear, measured values of strain at ultimate load ranged from 971 to 1878 microstrain. This corresponds to 4.3% to 8.9% of the capacity of the sheets that is 21 000 microstrain. For beams with shear failures, measured values of microstrain ranged from 4086 to 11 599, equivalent to 19.5% to 55.3% of the capacity of the sheets, respectively. The large variability of data can be attributed to the lack of uniformity in the strengthening process since the reinforcement is applied manually over the surface of the timbers.

Table 4.6 Horizontal forces in shear reinforcement of Beams SF

		Split			at P_{max}				at 40 kN				
Beam	Side	Length	k	P_{max}	Horiz. Force (theo)	micro strain	Force in reinf.	% of theo	Horiz. Force (theo)	mico strain	Force in reinf.	% of theo	Failure mode
		[mm]	[%]	[kN]	[kN]		[kN]	[%]	[kN]		[kN]	[%]	
Point of load at midspan													
y2-201	A	-	-	127.0	98.8	1452	31.5	31.9	31.2	470	10.2	32.7	Flexure
	B	-	-	127.0	86.6	1452	31.5	36.4	27.5	470	10.2	37.1	Flexure
y2-203	A	-	-	156.5	129.0	1878	40.7	31.6	33	468	10.1	30.8	Bearing
	B	-	-	156.5	126.9	1212	26.3	20.7	32.5	318	6.9	21.2	Bearing
y2-205	A	-	-	151.1	125.0	1559	33.8	27.0	33.1	378	8.2	24.8	Bearing
	B	-	-	151.1	124.7	1671	37.3	29.9	33.1	429	9.3	28.1	Bearing
y2-204	A	-	-	131.9	108.2	1012	21.9	20.2	33	307	6.7	20.2	Debond.B
y2-202	A	-	-	119.6	98.0	1460	31.7	32.3	33	458	9.9	30.1	Bearing
y1-206	A	-	-	130.1	109.2	971	21.1	19.3	33.7	310	6.7	19.9	Debond.B
y2-208	A	170	0.47	130.4	106.3	1494	33.4	31.4	32.7	444	9.6	29.4	Bearing
y2-209	A	190	0.48	134.1	109.6	1239	26.9	24.5	32.8	396	8.6	26.2	Debond. B
y2-204	B	600	0.53	131.9	161.8	8305	180.1	111.3	49.3	601	13.0	26.4	**Debond B**
y2-202	B	210	0.84	119.6	147.3	4784	103.7	70.4	49.6	727	15.8	31.8	Bearing
y1-207	A	875	0.54	129.8	182.3	7692	166.8	91.5	56.4	901	19.5	34.7	**Debond A**
y1-206	B	1540	0.57	130.1	266.2	11599	251.5	94.5	82.2	745	16.2	19.7	**Debond B**
y2-208	B	2000	0.80	130.4	217.1	8095	175.6	80.9	66.9	673	14.6	21.8	Bearing
y2-209	B	1200	0.50	134.1	221.1	4086	88.6	40.1	66.1	947	20.5	31.1	**Debond B**
y1-207	B	880	0.56	129.8	182.1	1894	41.1	22.6	56.2	310	6.7	12.0	Debond A

Table 4.7 Horizontal forces in shear reinforcement of Beams S (Load close to side A)

Beam	Side	Split Length	Split k	P_{max}	at P_{max} Horiz. Force (theo)	at P_{max} micro strain	at P_{max} Force in reinf.	at P_{max} % of theo	at 40 kN Horiz. Force (theo)	at 40 kN mico strain	at 40 kN Force in reinf.	at 40 kN % of theo	Failure mode
		[mm]	[%]	[kN]	[kN]		[kN]	[%]	[kN]		[kN]	[%]	
Point of load close to side A (second test)													
y2-109	B	1700	0.52	146.2	151.5	5829	126.4	83.4	41.5	997	21.6	52.1	**Debond.B**
y2-111	B	2300	0.52	99.9	132.7	-	-	-	53.3				*
y3-104	B	1615	0.71	193.6	169.8	6230	135.1	79.6	35.4	926	20.1	56.7	Bear.
y1-03	B	2180	*	140.8	144.5	6566	142.4	98.5	41.2	1490	32.3	78.5	Bear.
y2-110	B	800	0.54	170.5	104.3	-	-	-	24.7	-	-	-	Bear.
y3-03	B	2180	*	100.8	-	-	-	-	-	-	-	-	Bear.
y1-117	B	1160	0.45	-	-	-	-	-	-	-	-	-	
y2-108	B	1200	0.56	140.9	-	-	-	-	-	-	-	-	Dap
y2-114	B	1800	0.65	118.4	117.4	-	-	-	39.6	-	-	-	LP Bear.
y2-101	B	990	0.57	127.9	88.9	1221	26.5	29.8	27.8	340	7.4	26.5	Dap
y2-103	B	2050	0.51	132.6	158.6	3150	68.3	43.1	48	737	16.0	33.3	LP Bear.
y2-103	A	2170	0.38	132.6	231.6	4273	92.7	40.0	70.1	-1733	-37.6	-53.6	LP Bear.

* Not noted

Table 4.8 Horizontal forces in shear reinforcement of Beams S (Load close to side B)

Beam	Side	Split Length	Split k	P_{max}	at P_{max} Horiz. Force (theo)	at P_{max} micro strain	at P_{max} Force in reinf.	at P_{max} % of theo	at 40 kN Horiz. Force (theo)	at 40 kN mico strain	at 40 kN Force in reinf.	at 40 kN % of theo	Failure mode
		[mm]	[%]	[kN]	[kN]		[kN]	[%]	[kN]		[kN]	[%]	
Point of load close to side B (first test)													
y2-16	A	2130	0.47	148.1	180.1	12329	267.4	148.5	48.79	945	20.5	42.0	**Debond.A**
y2-109	B	1700	0.52	172.1	355.9	7120.5	154.4	43.4	82.82	909.5	19.7	23.8	Bear.
y2-111	B	2300	0.52	80.1	147.0	2825.3	61.3	41.7	73.78	1015	22.0	29.8	Dap
y3-104	B	1615	0.71	141.9	241.4	4423.5	95.9	39.7	68.09	658	14.3	21.0	LP Bear.
y1-03	B	2180	*	159.1	330.2	8599.5	186.5	56.5	83.13	1014	22.0	26.5	Bear.
y2-110	B	800	0.54	158.9	291.5	10324	223.9	76.8	73.98	1211	26.3	35.5	Bear.
y3-03	B	2180	*	137.0	-	-	-	-	-	-	-	-	Bear
y1-117	B	1160	0.45	122.4	254.0	8930	193.7	76.2	83.45	1098	23.8	28.5	Flexure
y2-108	B	1200	0.56	160.6	347.8	6144	133.2	38.3	86.67	382	8.3	9.6	Bear
y2-114	B	1800	0.65	131.4	238.5	6257.5	135.7	56.9	72.79	1391	30.2	41.4	**Debond.B**
y2-101	B	990	0.57	103.3	215.3	2122	46.0	21.4	84.02	714.5	15.5	18.4	Bear.
y2-103	B	2050	0.51	115.1	220.9	2730	59.2	26.8	77.43	-11	-0.2	-0.3	LP Bear.
y2-103	A	2170	0.38	115.1	220.9	9362	203.0	91.9	77.43	2565	55.6	71.8	LP Bear.

* Not noted

In the beams from complementary data, three shear failures by debonding of the shear reinforcement were observed. Shear failures occured at values of 5829, 6257.5, and 12329 microstrain, that corresponds to 27.9, 29.86, and 58.8 % of capacity of the sheets. It can also be seen that other beams developed high values of microstrain in the shear reinforcement without debonding failures such as, Y1-03B, Y2-110B and Y1-117B, with microstrain values of 8599.5, 10324 and 8930, respectively. Two of these beams had splits close to the middle of the height of the beam with height values of 0.54 and 0.45, and splits that extended far into the beam. The analysis will focus on the weakest samples that failed by debonding of shear reinforcement at even smaller stresses.

4.3 DURABILITY TEST

For this test, eight full-scale, creosote treated, previously tested to failure beams (Beams S and Beams SF), were visually inspected and then subjected to 4 months of cycles of weekly changes of temperature and relative humidity (R.H.) ranging from 20 to 40°C and 25 to 85% R.H. Detailed information about the cycles can be seen in Table 3.4. Visual evaluation of new or additional debonding of the shear reinforcement was done after each monthly set of cycles. Some of these beams exhibited debonding of one or more of the four shear reinforcing sheets due to its previous test. Other beams had modes of failure other than shear and the shear reinforcement was still firmly attached to the treated surface of the wood. The original condition of the beams was assessed at the beginning

of the test. The objective of this test was to investigate the effect of temperature and humidity on durability of fully or partially bonded sheets.

The beams used for this experiment were taken from an exterior environment where they were only protected by a roof. The week prior to the test, the beams were exposed to high values of exterior relative humidity ranging from 70 to 100% R.H. At the end of the test, the beams were subjected to a week of controlled relative humidity of 25%. Table 4.9 reports values of moisture content of the beams taken at the beginning and ending of the test. Reported values ranged from 13.4 to 18.5% before the test, compared to 12.8 to 18.05% after the test. Moisture content of the beams was only reduced up to 2.1%; this is an indication of the effectiveness of the creosote treatment in preventing large changes of moisture content of the treated elements, even though most of them had splits.

Table 4.9 Moisture content of beams before and after durability test

	Moisture content [%]		Variation
	30-Aug-04	07-Jan-05	[%]
y2-202	15.15	13.90	1.3
y1-206	15.00	12.95	2.1
y1-207	15.15	14.10	1.1
y2-209	13.50	13.05	0.4
Y1-03	13.40	13.80	-0.4
y1-116	14.20	12.80	1.4
y1-117	15.85	14.70	1.2
115	18.45	18.15	0.3

Tables 4.10, and 4.11 report all observations of debonding of the shear reinforcement at the beginning of the test and the additional debonding, if any, after each monthly set of cycles. Additional debonding was measured in millimeters in the direction parallel to the reinforcement fibres (y deb.), and the direction perpendicular to the fibres (x deb.). From Tables 4.10, and 4.11, it can be observed that some of the reinforcing sheets with debonding at the beginning of the tests exhibited additional debonding at the end of last two sets of cycles. Debonding of these samples ranged from 0 to 14.4%. No additional debonding was observed at the end of the test for fully bonded reinforcing sheets. The same results were observed in the two groups of beams regardless of the fact that the beams were reinforced at different times and some differences in the quality of the reinforcement process were observed.

The durability test constitutes an initial assessment based on visual inspection and it is not conclusive on the long-term performance of the bonding of the external reinforcement. Nevertheless, the observations are evidence that weather cycles of changing temperature and relative humidity could have a negative effect on the bonding characteristics of GFRP external reinforcement, especially if the sheets are initially debonded in certain areas.

The cycles used in this research were stopped too early to find more problems with the sheets. It is recommended that any future cycling takes at least 12 months to evaluate the effect on the strengthened samples.

Table 4.10 Results from the durability test. Part I

		Maximun additional debonding [mm]				Total additional debonding [mm]			
	30-Aug-04	06-Oct-04	04-Nov-04	27-Nov-04	07-Jan-05	x deb. [mm]	y deb. [mm]	x deb. [%]	y deb. [%]
y2-202	SIDE D								
	A slightly deb	0	0	0	0	0	0	0.00	0.00
	B slightly deb	0	0	20	0	0	20	0.00	**3.54**
	SIDE E								
	A slightly deb	0	0	0	60	60	0	**14.14**	0.00
	B ok	0	0	0	0	0	0	0.00	0.00
y1-206	SIDE D								
	A ok	0	0	0	0	0	0	0.00	0.00
	B debonded	0	0	0	0	0	0	0.00	0.00
	SIDE E								
	A ok	0	0	0	0	0	0	0.00	0.00
	B debonded	0	0	0	0	0	0	0.00	0.00
y1-207	SIDE D								
	A debonded	0	0	0	0	0	0	0.00	0.00
	B ok	0	0	0	0	0	0	0.00	0.00
	SIDE E								
	A slightly deb	0	0	0	0	0	0	0.00	0.00
	B ok	0	0	0	0	0	0	0.00	0.00
y2-209	SIDE D								
	A ok	0	0	0	0	0	0	0.00	0.00
	B debonded	0	0	0	0	0	0	0.00	0.00
	SIDE E								
	A ok	0	0	0	0	0	0	0.00	0.00
	B debonded	0	0	0	0	0	0	0.00	0.00

Table 4.11 Results from the durability test. Part II

			Maximun additional debonding [mm]				Total additional debonding [mm]			
		30-Aug-04	06-Oct-04	04-Nov-04	27-Nov-04	07-Jan-05	x deb [mm]	y deb [mm]	x deb [%]	y deb [%]
y1-03	SIDE D									
	A	ok	0	0	0	0			0.00	0.00
	B	slightly deb	0	0	0	28	28	8	**6.60**	**1.41**
	SIDE E									
	A	ok	0	0	0	0	0	0	0.00	0.00
	B	ok	0	0	0	0	0	0	0.00	0.00
y1-116	SIDE D									
	A	debonded	0	0	0	0	0	0	0.00	0.00
	B	ok	0	0	0	0	0	0	0.00	0.00
	SIDE E									
	A	debonded	0	0	0	0	0	0	0.00	0.00
	B	slightly deb	0	0	0	0	0	0	0.00	0.00
y1-117	SIDE D									
	A	ok	0	0	0	0	0	0	0.00	0.00
	B	ok	0	0	0	0	0	0	0.00	0.00
	SIDE E									
	A	ok	0	0	0	0	0	0	0.00	0.00
	B	ok	0	0	0	0	0	0	0.00	0.00
115	SIDE D									
	A	ok	0	0	0	0	0	0	0.00	0.00
	B	slightly deb	0	0	0	10	10	0	**2.36**	0.00
	SIDE E									
	A	ok	0	0	0	0	0	0	0.00	0.00
	B	slightly deb	0	0	0	10	10	5	**2.36**	**0.88**

CHAPTER 5

DATA ANALYSIS

5.1 RELIABILITY ANALYSIS

The safety of a structural element depends on the variability implied in the strength of the element and the applied loads. The probability of the applied forces exceeding the resistance of the structure can be assessed by means of the safety index, β; it is the first order measure of the reliability of the component. The analysis using the safety index is based on the assumption that the reliability of a component can be expressed by the mean and the standard deviation of the resistances and load effects. The safety index, β, can be calculated using equation 5.1.

$$\beta = \frac{\mu_R - \mu_S}{\left(\sigma_R{}^2 + \sigma_S{}^2\right)^{0.5}} \tag{5.1}$$

Where μ_R is the mean of the resistance forces, μ_S is the mean of the applied forces, σ_R is the standard deviation of the resistance forces, and σ_S is the standard deviation of the applied forces. The equation is based on the assumption that failure takes place when the resistance of the elements is exceeded by the applied loads. According to Mufti et al. (1996), the first

generation of probabilistic-based design codes are calibrated to β = 3.5. This target reliability index, β, represents the required level of safety that must be provided by the structural capacity of a bridge component; it depends upon the life safety and economic consequences of failure.

The current reliability analysis was made using the resistance of the samples tested in this experimental program, and bar reinforced samples tested by Amy (2004). Statistical parameters for calculating the mean and standard variation of applied loads are found in the Canadian Highway Bridge Design Code CHBDC commentary (2000).

Amy (2004) calculated the maximum factored applied moment for a beam with the same dimensions used in the present study. A value of 37.26 kN.m of maximum moment was obtained based on the CL-625 design truck using the CHBDC (2000). The calculations were made using the heaviest axel loading at midspan, two lanes of traffic, and a dynamic load allowance factor of 0.4. The mean and standard deviation of the applied moment were calculated by multiplying the obtained value by the bias factor and coefficient of variation from Table CA. 4.2.1.1 of the CHBDC commentary (2000). The factors represent the variation of the applied loads obtained from statistical data of a survey conducted in Saskatchewan in 1995. The standard deviation can be calculated by multiplying the mean value by the coefficient of variation and the bias factor is used to calculate the mean. Values of 0.84 and 0.0296 for bias factor and coefficient of variation respectively, were obtained from Table CA 4.2.1.1. From

these values, a mean applied moment equal to 31.3 kN.m and a standard deviation of 0.926 are calculated. The values of mean and standard deviation for applied and resistant moments are shown in Table 5.1. In the table, the safety index of the beams tested in this research program can be compared with safety index of the bar-reinforced beams previously tested by Amy (2004). The reinforcement ratios of the beams are shown in Table 4.3.

Table 5.1 Reliability index of the externally reinforced samples compared with bar-reinforced samples tested by Amy (2004)

	Mean [kN.m]	Standard Deviation	β
Loading	31.30	0.926	N/A
Beams C	103.40	19.70	3.66
Beams B	126.70	21.70	4.40
Beams SF	113.45	10.51	7.84

The safety index of both bar-reinforced specimens and sheet-reinforced specimens satisfy the desired value of 3.5. The sheet-reinforced specimens exhibited a large value of reliability index of 7.84, compared with a value of 4.40 for the bar-reinforced specimens. The high value of the reliability index was obtained because of the low variability in the results of the sheet–reinforced specimens. This variability is represented by the low value of standard deviation of 10.51, compared with 21.7 of the bar-reinforced specimens.

The externally reinforced specimens can be considered safe to resist the loads considered because they had an excellent behaviour in terms of variability.

Nevertheless, the conclusions of this reliability analysis are limited by the small number of full-scale reinforced samples that were tested.

5.2 HORIZONTAL SHEAR FORCES

A simplified analysis has been carried out to calculate the horizontal shear forces that act through the depth of the shear reinforced portion of the beams. These horizontal shear forces along the grain of the timber are critical at split depth producing debonding of the shear reinforcement in the split beams when the splits are close to midheigth. Calculations are based on a simplified analysis that does not take into account the more complex interactions in the reinforced system; therefore it is not intended to be an exact calculation. The forces calculated using this method were compared with experimental data to determine the proportion of that force that is supported by the reinforcement. As a result, the capacity of a strengthened split beam can be assessed.

The proposed calculations of theoretical horizontal shear forces in the section are based on assumptions that are the simplification of a more complex behaviour. It first assumes that plain sections remain plane during bending and that the radius of curvature of the top and bottom portions of the split beams is the same; this is confirmed by the tests where no separation between top and bottom portions of split beam was observed. Another assumption is that the material is elastic and homogeneous which is not accurate because timber develops its resistance in the inelastic range and it is not a homogeneous material. This method also

further assumes that the shear reinforced portion of the beam is rigid. This assumption describes the initial behaviour when no slip deformation along the length of the split occurred. Accordingly, calculated horizontal forces correspond to the initial linear behaviour. Shear reinforcement develops its strength when large slip deformations are present along the split that slowly debonds the reinforcement until the final debonding failure takes place.

The proposed method is based on similar calculations of horizontal shear forces presented by Huggins et al. (1966). For the shear reinforced portion of a split beam, the forces in the plane of the split were calculated by obtaining the distribution of flexural stresses in vertical planes on opposite sides of the shear reinforcement. The distribution of bending stresses at inner side of the shear reinforced portion can be calculated by solving the system shown in the free body diagram of Figure 5.1.

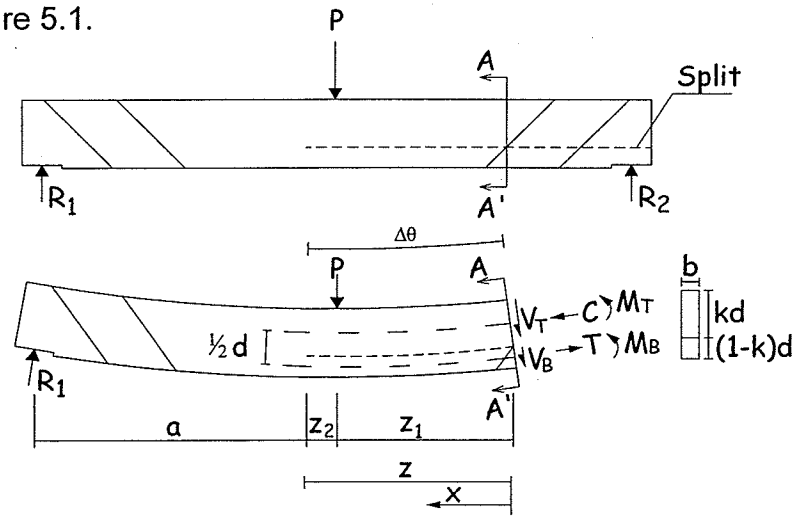

Figure 5.1 Free body diagram

Figure 5.1 shows the free body diagram of a portion of the beam at one side of plane A-A' where the split extend beyond the shear reinforced portion of the

beam. The location of the split, k, is measured from the top of the section and is expressed as a fraction of the beam's height, d. The beam has a width b and the split extends a distance equal to z beyond plane A-A'. The free body diagram shows the applied force P and the reaction at the opposite support R1. It also shows the forces acting on top and bottom portions of the split beam. The top portion of the beam is subjected to the shear force V_T, moment M_T and compression force C, and the bottom portion is subjected to shear force V_B, moment M_B and tension force T.

No vertical separation of the split was observed during the test, so top and bottom portions of the element are assumed to have the same radius of curvature, ρ, thus:

$$\frac{1}{\rho} = \frac{M_T}{EI_T} = \frac{M_B}{EI_B} \tag{5.2}$$

Equation (5.2) gives a relationship between bending moments acting on top and bottom portions of the split beam related to their moments of inertia. For beams with flexural reinforcement, the moment of inertia of the bottom portion of the split element is calculated using the transformed section to include the effect of the reinforcement. Equation (5.3) is the equilibrium of the section, proposed by Huggins et al. (1964). Calculating equilibrium of moments at the point of action of tensile force T and shear forces V_T and V_B gives the equation:

$$R1 \cdot (a + z_1 + z_2) - P(z_1) - M_T - M_B - C\frac{d}{2} = 0 \qquad (5.3)$$

Equation (5.7) is necessary to solve the system. It is found by calculating the angle $\Delta\theta$ which is the change in slope of the deformed curve. A value of $\Delta\theta$ can be obtained by subtracting the change in length at the centre of top portion of the split section ($\frac{-C \cdot z}{A_T \cdot E}$) from the change in length at the centre of bottom portion of the split section ($\frac{+T \cdot z}{A_T \cdot E}$), and dividing it by the distance between centres, $d/2$.

$$\Delta\theta = \frac{1}{d/2}\left[\frac{Cz}{A_T E} + \frac{Tz}{A_B E}\right] \qquad (5.4)$$

The angle $\Delta\theta$ can also be calculated by the integral of the moment between point A and point B in Figure 5.2. Moments acting on top and bottom portions of the beam are proportional, so $\Delta\theta$ can be calculated using the moment acting on top portion $M_T(x) = M_T + V_T \cdot x$.

$$\Delta\theta = \frac{1}{EI_T}\int_0^z (M_T + V_T \cdot x)\,dx \qquad (5.5)$$

$$\Delta\theta = \frac{1}{EI_T}\int_0^{z_1} (M_T + V_{T2} \cdot x)\cdot dx + \int_0^{z_2} (M_T + V_{T2} \cdot z_1 - V_{T1} \cdot x)\cdot dx \qquad (5.6)$$

Equation (5.5) and Equation (5.6) can be then expressed as follows:

$$\frac{2z}{d \cdot E}\left[\frac{C}{A_T} + \frac{T}{A_B}\right] = \frac{1}{EI_T}\int_0^z (M_T + V_T \cdot x) \cdot dx \qquad (5.7)$$

Solving the system of three equations (5.2, 5.3, and 5.7), the distribution of stresses at the inner face of shear reinforced portion (A-A') can be found. Figure 5.3 shows the distribution of forces in section CAEF. The distribution of stresses at the inner side CA corresponds to the calculated values C and M_T of Figure 5.1. The distribution of stresses in the outer side EF has a resultant horizontal force equal to zero because it corresponds to the unrestricted end portion of the split beam. A force V' should be present to equilibrate horizontal forces in the section. Accordingly, the force V' should be equal to the computed compression force C found in previous calculation and Figure 5.1.

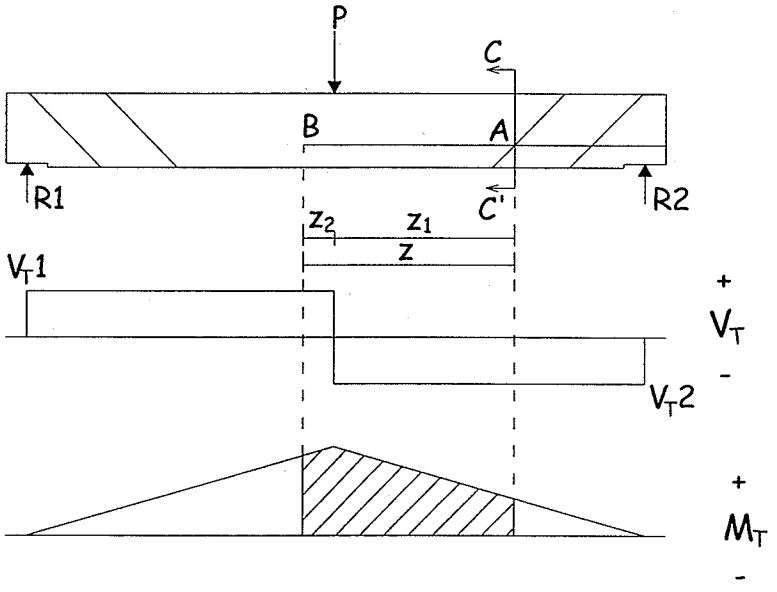

Figure 5.2 Shear and moment diagrams of top portion of split beam

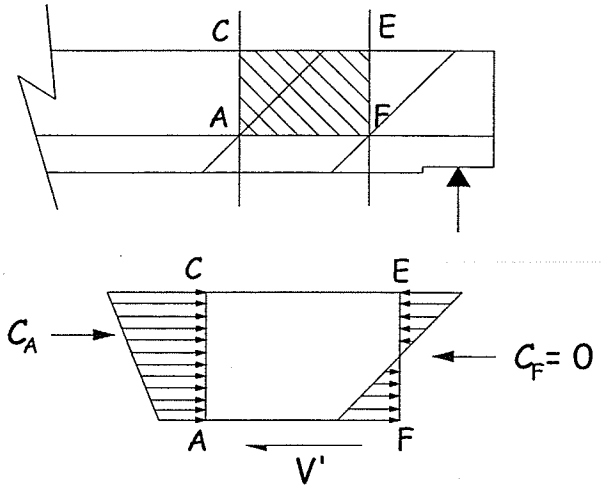

Figure 5.3 Horizontal force V' on free body diagram ACEF

The horizontal shear force, V', can be found at different heights of the section using the distribution of stresses shown in Figure 5.3. Their values can be compared with experimental values of stresses in reinforcement sheets to determine the proportion of the force that is supported by the shear reinforcement. Nominal horizontal shear forces can be calculated by computing the shear flow, q, of the section at any height.

$$q = \frac{VQ}{I} \tag{5.8}$$

For this equation, V is the vertical shear force in the section, Q is the first moment of area of the section at height of calculation and I is the moment of inertia of the section. The nominal horizontal shear force can be calculated by multiplying the shear flow, q, by the length AF shown in Figure 5.3 which is the length of the shear reinforced portion of the beam. Nominal horizontal shear forces were calculated at midheight for non-split beams. Horizontal shear forces and nominal horizontal shear forces were calculated for split beams at split height.

5.1.1 Theoretical forces acting on shear reinforced portion of the beams

Using equations 5.2, 5.3, and 5.7, it is possible to analyze the effect of the split size and depth on the amount of horizontal shear force resisted by the shear reinforced portion of a split beam for different configurations of load. A graphical solution has been created by constructing a chart that allows quick calculation of theoretical horizontal shear forces acting on the reinforced portion of the split element. The chart has been developed for the proposed reinforcement scheme of 300 mm straps at 45°. The chart was developed using an iterative procedure that calculates values of relationship between shear force and applied load. Calculations are made by solving the system of equations 5.2, 5.3 and 5.7 shown before; the iteration process gives values for each combination of split length and split height. Figures 5.4, 5.5, and 5.6, show the effect of splits on the relationship between horizontal shear force and applied load for point loads at midspan, at quarter span close to the split end, and at quarter span far from split end respectively. The horizontal axis contains the length of the split, while the vertical axis shows the ratio of horizontal shear force to load. The graphs are calculated for depth of the split kd, with the values from 0.3 to 0.8. This depth is measured from the top fibre of the beam. It is possible to observe from the graphs that different split lengths are more critical depending on the point of application of the load. The same graphs were constructed for 200 x 600 x 10400 mm beams reinforced for shear with 600 mm straps inclined at 45° with respect to the longitudinal plane. The graphs are shown in Figures 5.7, 5.8, and 5.9.

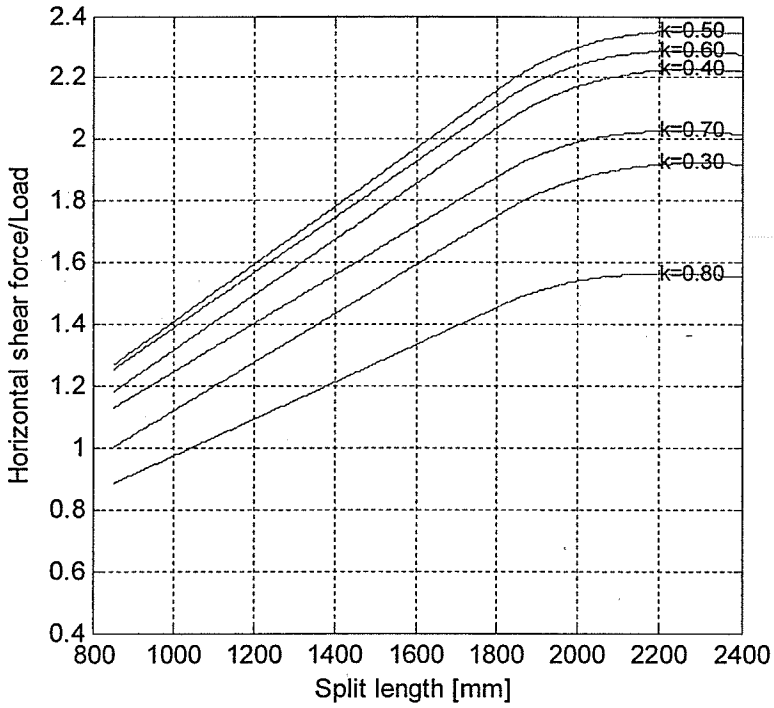

Figure 5.4 Horizontal shear forces for 3650mm long beams loaded at midspan

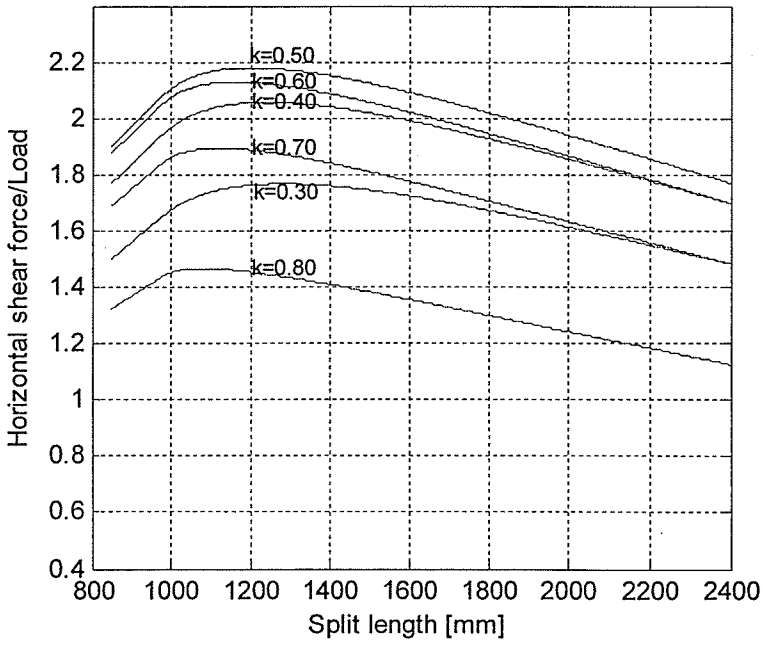

Figure 5.5 Horizontal shear forces for 3650mm long beams loaded at quarterspan with point load close to split end

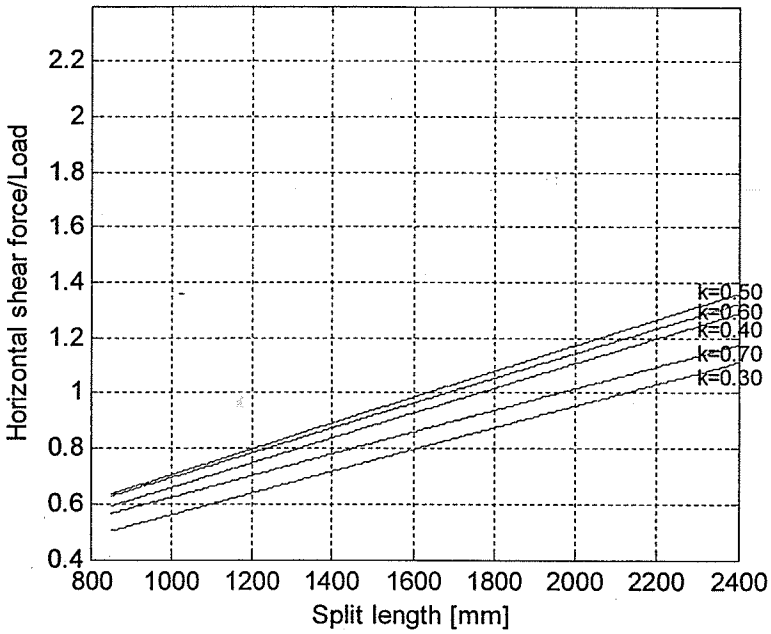

Figure 5.6 Horizontal shear forces for 3650mm long beams loaded at quarterspan with point load far from split end

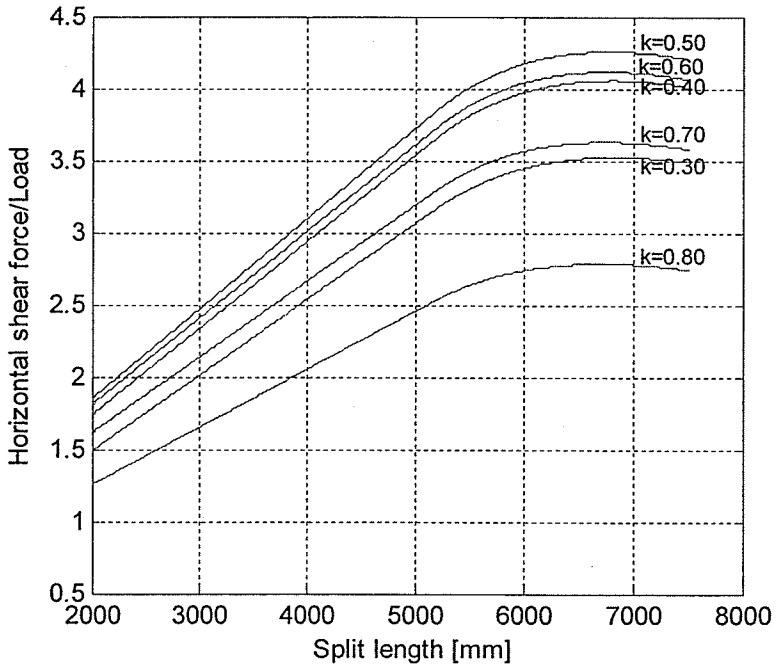

Figure 5.7 Horizontal shear forces for 10,000mm long beams loaded at midspan.

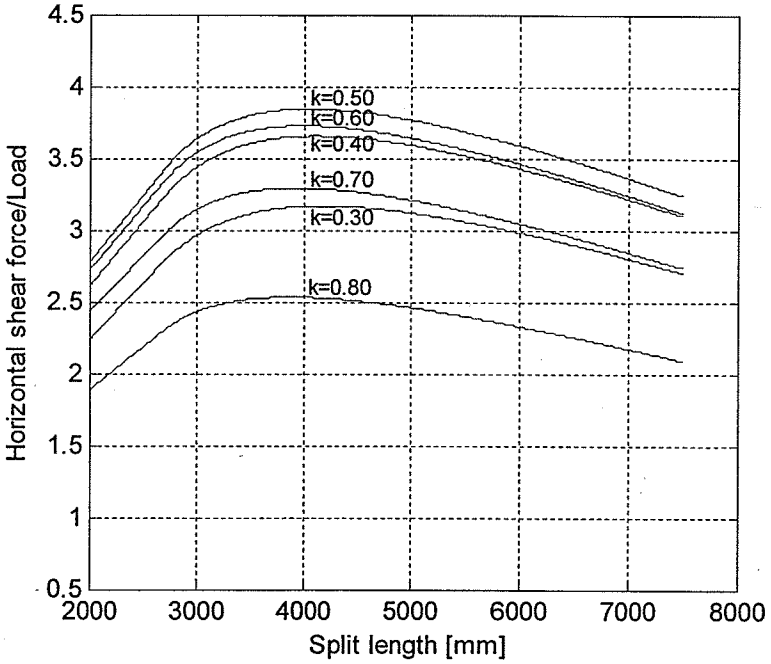

Figure 5.8 Horizontal shear forces for 10,000 mm long beams loaded at quarterspan with point load close to split end

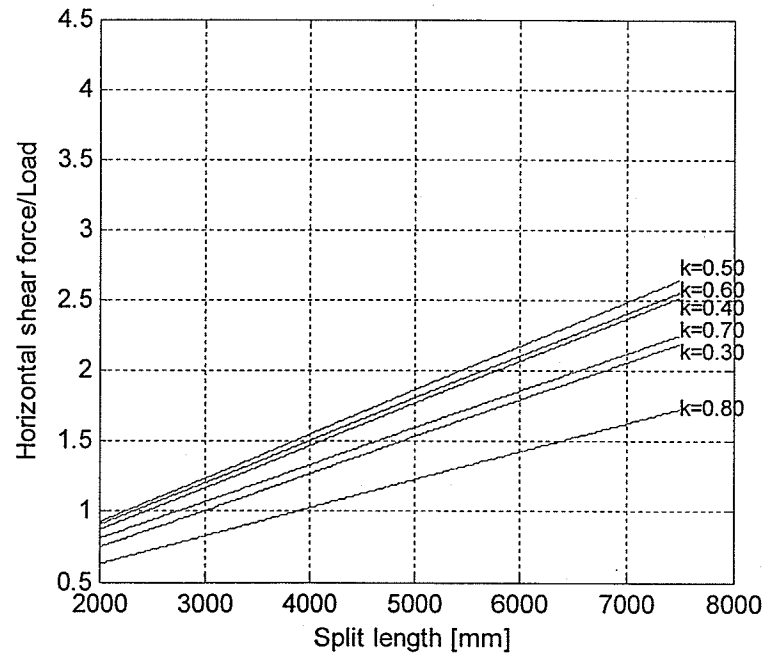

Figure 5.9 Horizontal shear forces for 10,000 mm long beams loaded at quarterspan with point load far from split end

An assessment of the point load likely to produce failure can be made by comparing horizontal shear forces obtained from the chart with horizontal shear forces associated to debonding failures in tested beams. Comparing the experimental data from from Beams S and SF, it is observed that shear failures took place at theoretical horizontal shear forces ranging from 151.5 kN to 266.2 kN (Tables 4.6, 4.7, and 4.8). It is a wide range, however, calculated values for both tests varied in the same range regardless of the difference in loading pattern.

The point load at certain location likely to produce debonding of the shear reinforcement for a given beam can be obtained by using the respective chart and the theoretical horizontal shear forces mentioned above. Having the dimension of the beam (3650 or 10 400), and the size and position of the split, the ratio of horizontal shear forces over applied load can be obtained from the chart. The critical point loads can be calculated by multiplying the ratio obtained from the chart by 150 kN, that is the lower value of shear force associated with failures by debonding in the tested samples. If the calculated load is larger than the effects of applied load, alternative strengthening scheme need to be implemented. The size and position of splits that produced shear failures should be taken into account in the analysis, that aspect is explained at the end of section 5.1.3.

5.1.2 Experimental stresses acting on shear reinforcing sheets

Figure 5.10 shows experimental forces acting in the shear reinforcement for some of the non-split beams or beams with small checks or splits (grade No.1 and better). Experimental forces in reinforcement were calculated as the horizontal component of the force corresponding to the strain measured by strain gauges above and below the split. Experimental forces in the reinforcement ranged from 20% to 37% of nominal shear forces in the section. These percentages correspond to the reinforcement contribution to resist the nominal horizontal shear forces; the remaining portion of the force is resisted by the timber. Experimental forces in shear reinforcement of non-split beams increase linearly with the load increment up to ultimate load, when failure is produced by reasons other than shear.

Figure 5.11 presents a comparison between calculated horizontal shear forces in split beams, nominal horizontal shear forces and experimental forces in shear reinforcement. Experimental forces in shear reinforcement of beams with split ends exhibited an initial linear behaviour followed by a curved portion. The curved portion coincides with observations of slip deformation starting between the two portions of the split element. For some of the beams, failure is produced by debonding of the shear reinforcement after slip deformation; the maximum amount of slip observed during test was 8 mm. The initial linear values of experimental forces in the reinforcement represent 19.7 to 34.7% of reinforcement contribution to resist calculated horizontal shear forces.

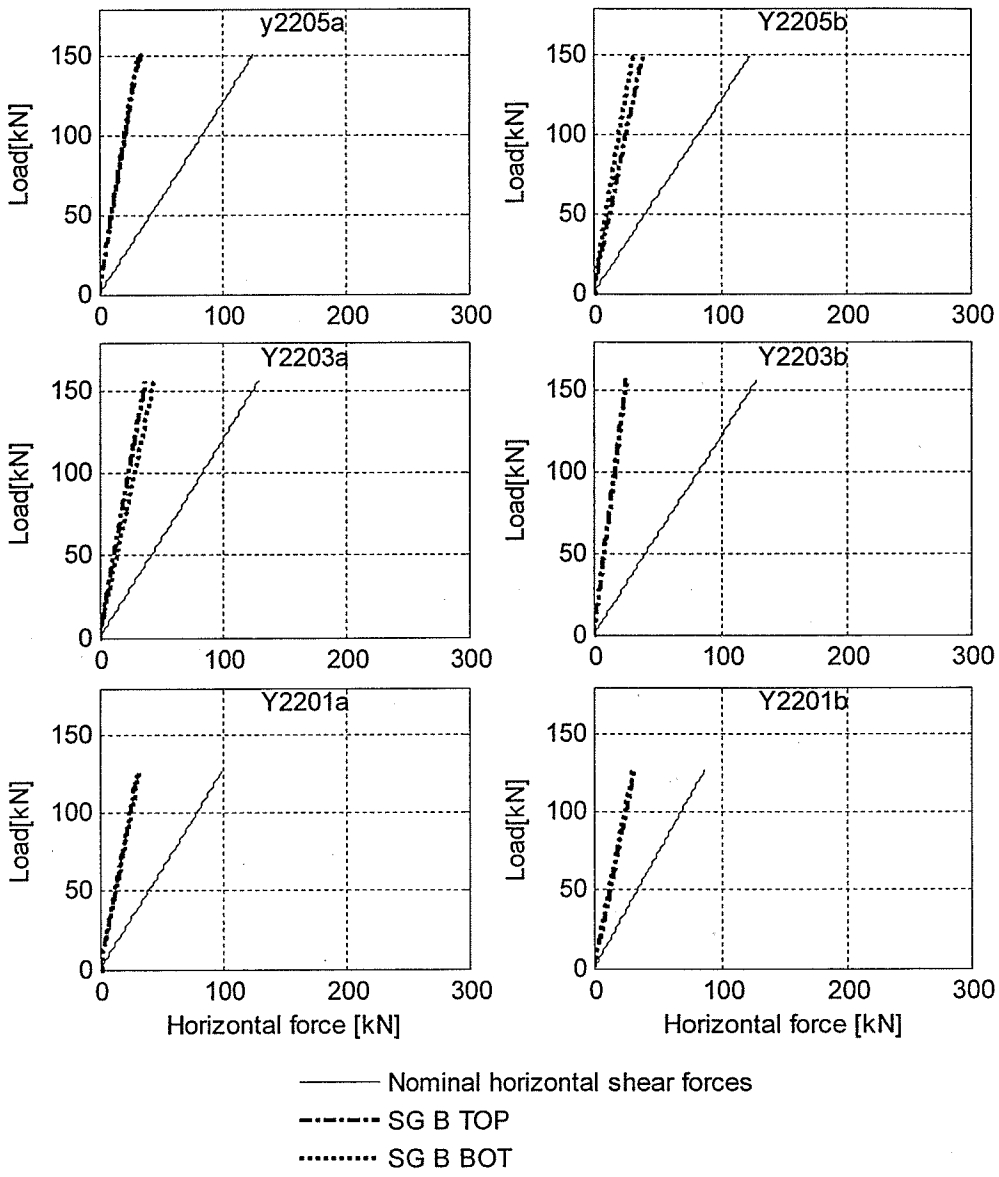

Figure 5.10 Nominal horizontal shear forces and experimental forces in the shear reinforcement of some non-split beams.

Percentage values of reinforcement contribution to resist horizontal shear forces are shown in Table 4.6. These values were calculated at ultimate load and at a load of 40 kN, that corresponds to a point within the initial linear behaviour for all

the beams, before slip deformations are produced. Nominal horizontal shear forces calculated using the concept of shear flow are also shown in Figure 5.11; nominal forces do not have similar proportions with experimental forces in the reinforcement for different beams. A better relationship between forces in the section and forces resisted by the reinforcement can be established using the simplified method explained before.

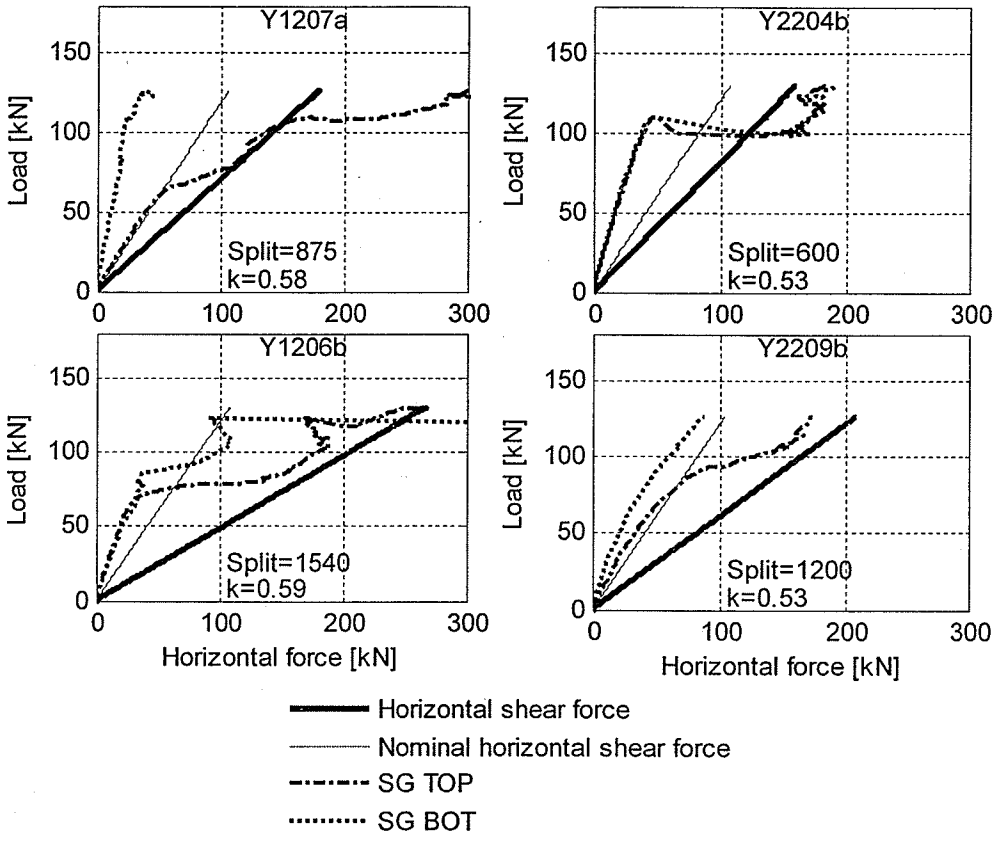

Figure 5.11 Horizontal shear forces, nominal horizontal shear forces and experimental forces in the shear reinforcement

Beams Y2-204 and Y2-202 had short splits extending from one end of the beams to a point within the shear reinforced portion of the beams as shown in Figure 5.12. An approximation of the horizontal shear force between point A and point F

was calculated by using the distribution of stresses at the inner side of the shear reinforced portion of the beam and considering that the resultant force at the outer side is zero. For these beams, the measured portion of the force carried by the reinforcement ranged from 26.4 to 31.84% of the calculated horizontal shear force.

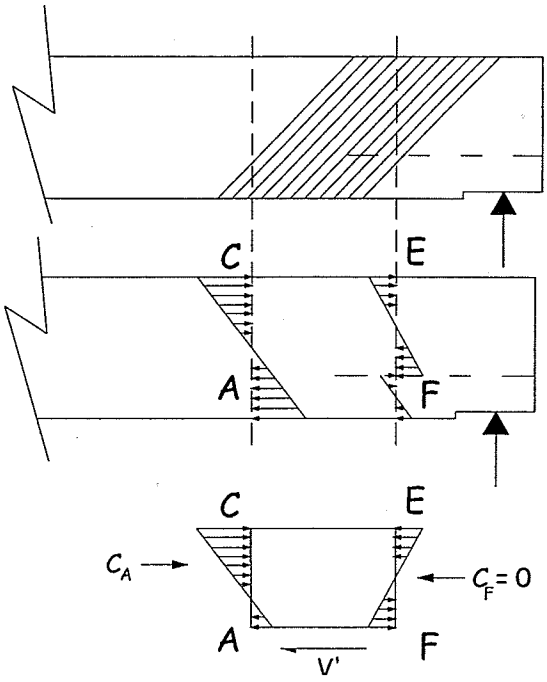

Figure 5.12 Horizontal force V' on beams with small splits

5.1.3 Calculated horizontal shear forces of additional samples.

Analysis of the data collected from the previous research by Hay (2004), revealed similar proportions of horizontal shear force taken by the shear reinforcement; a summary of the results can be seen in Tables 4.7 and 4.8. For split beams in the first test, initial values of experimental forces in the shear reinforcement ranged from 18.4 to 42 % of calculated horizontal shear forces. Some unusual higher

and lower values were also observed. For most non-split beams, the sheet contribution ranged from 17.9 to 28.8%. The proportions of horizontal forces taken by the shear reinforcement for split and non-split beams were similar. This behaviour shows that the major part of the shear forces is resisted by the timber itself even if the beams have long splits. The first and second tests on each beam were compared revealing higher proportions of forces resisted by the sheets in the second test. This larger portion of forces taken by reinforcement during the second test can be explained by complete separation between split portions of the beam during the test. Residual wood fibres were broken during the first test resulting in less resistance of the timber and larger contribution of the reinforcement in the second test.

Beam Y2-109 was instrumented with 5 strain gauges along the depth of the shear reinforcement. A profile of the experimental forces in the reinforcement at an applied load of 40 kN is shown in Figure 5.13 and it is compared with a profile of calculated horizontal shear forces using the method by Huggins (1966). The figure shows similar profile of forces along the depth of the element for the experimental forces in the shear reinforcement and the calculated forces in the section. There is a peak of force at the location of the split.

Shear failure was not critical for the beams with short splits or splits at low heights. Calculated values of horizontal force were high for some of the beams that exhibited failure modes different than shear; this is the case of beams with splits at a low height (0.7d or 0.8d) or splits shorter than a quarter of the span.

For beams with long splits located at low heights, debonding failure was not critical since the proposed reinforcement method provides anchorage at the bottom of the beam by wrapping the reinforcement around the section. For beams with splits shorter than quarter of the span, debonding failures are not critical because of the smaller slip deformation along the split.

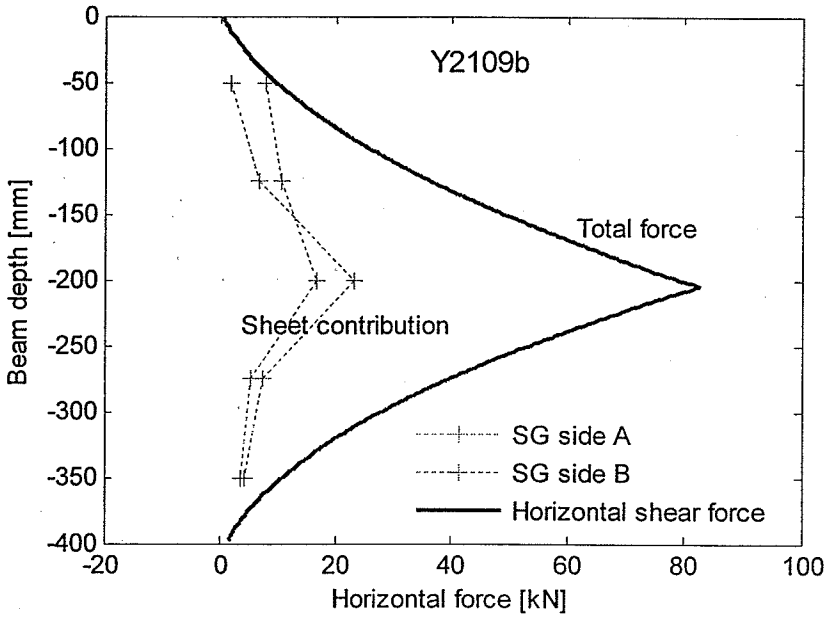

Figure 5.13 Profile of forces at a load of 40 kN

CHAPTER 6

CONCLUSIONS

A research program was developed at the University of Manitoba to study different aspects of retrofitting aged timber stringers using external reinforcing GFRP sheets. The research program was composed of three tests: direct shear test, bending test of full-scale specimens and durability test.

The direct shear test dealt with an isolated aspect of the overall behaviour of reinforced timber beams; it was designed to evaluate and compare various reinforcing schemes of FRP shear reinforcement for split beams. The direct shear test revealed that the 30° configurations of shear reinforcement were stronger than 45° and 90° configurations for both FRP reinforcing bars and FRP reinforcing sheets. The smaller angle of the reinforcement causes the load to be more parallel to the direction of the load-resisting fibres producing better results. The smaller angle patterns were also more rigid than the larger angle ones. The 30° reinforcing configurations experienced smaller deformations at ultimate.

External reinforcement patterns exhibited 77% to 100% higher mean capacity to resist horizontal shear compared with bar reinforcement patterns. However, the results of this test are non-conservative for the external reinforcement because

the wood used was not creosote-treated. Lower capacities of externally reinforced specimens should be expected for creosote-treated timber.

The external 30° reinforcement configuration uses a larger length of reinforcing sheets. This configuration of reinforcement developed a larger proportion of its capacity before debonding. It indicates that resistance of the external reinforcement could be increased by providing larger development lengths. This could be done by providing additional anchorage strips.

Full-scale aged timber stringers retrofitted for shear and bending with GFRP sheets were tested in 3-point bending. The proposed reinforcement pattern produced mean strength improvement of 10.8% for strengthened beams compared with control beams and stiffness improvement of 8.8 to 60.5% depending on the level of beam damage in the form of longitudinal splits.

According to the results obtained from the bending test, aged beams retrofitted using the proposed external reinforcement pattern are safe to resist the live loads corresponding to the CL-625 design truck of the CHBDC code. The externally reinforced elements tested exhibited a reliability index of 7.84, which is larger then the minimum desirable value of 3.5. This high value of the safety parameter was attained because of the low variability of resistance between the tested beams. The conclusions in this respect are limited because of the small quantity of old full-scale reinforced beams that can be tested due to practical restrictions.

The tested beams reinforced with the proposed pattern and with splits close to midheight and longer than beam depth, exhibited shear failures by debonding of the shear reinforcement. These split beams are the weakest beams having failures at smaller loads than non-split reinforced beams; their mean shear strength was 2.46 MPa, with a minimum value of 2.43 MPa. Calculated horizontal shear forces in the shear reinforced portion of the beams can be compared with measured forces on reinforcement sheets. Similar proportions of experimental forces in the reinforcement to calculated forces acting in the section were obtained for different loading configurations. The proportion of the reinforcement to resist experimental shear forces ranged from 18.4 to 42 % at 40 kN corresponding to behaviour previous to slip deformation and ranged from 40.1% to 148.5% at ultimate, after slip deformation took place. Shear failures with debonding of the reinforcement took place at theoretical horizontal shear forces ranging from 151.5 to 266 kN.

Shear failure was not critical for the beams with splits shorter than a quarter of the span or splits at low heights (0.7d or 0.8d). For beams with long splits located at low heights, debonding failure was not critical since the proposed reinforcement method provides anchorage at the bottom of the beam by wrapping the reinforcement around the section. For beams with splits shorter than quarter of the span, debonding failures are not critical because of the smaller slip deformation along the split.

The observations made in the durability test indicate that cycles of changing temperature and moisture content could have a negative effect on the bonding characteristics of GFRP external reinforcement. The shear reinforcing sheets evaluated in this test without original debonding exhibited a good performance under the chosen weathering or aging cycles, nevertheless, shear reinforcing sheets with some extent of original debonding exhibited additional debonding after two months of cycles of changing temperature and relative humidity.

The durability test constitutes an initial assessment based on visual inspection and it is not conclusive on the long-term performance of the bonding of the external reinforcement. Observations indicate that long-term performance of bonding of external reinforcement should be investigated in more detail to ensure that the reinforced beams will resist the harsh environmental conditions to which they would be exposed to during their service life.

Results from the direct shear test and bending test indicate that GFRP sheets can be effectively used in the retrofitting of aged split timber stringers. The external reinforcement produces important improvements in strength and stiffness of the elements even with low values of reinforcement ratio. The combined effect of shear and bending external reinforcement, bridges the defects of the aged beams producing the positive effect of reducing the variability in results.

REFERENCES

Abdel-Magid, B., and Dagher, H.J., and Kimball, T. (1994) "The Effect of Composite Reinforcement on Structural Wood" Proceedings of the 3rd Materials Engineering Conference, San Diego, CA, 417-424.

Amy, K., and Svecova, D. (2004) "Strengthening of dapped timber beams using glass fibre reinforced polymer bars" Canadian Journal of Civil Engineering, 31:943-955.

Amy, K. (2004) "Reinforcing of Dapped Timber Stringers with GFRP Bars" Thesis presented to the University of Manitoba, Winnipeg, Manitoba, Canada, in partial fulfillment of the requirements for the degree of Master of Science in Civil Engineering.

ASTM (1999) "Standard Test Methods of Static Tests of Lumber in Structural Sizes" D 198-99, Philadelphia, PA.

ASTM (1996) "Standard Test Method for Multiple-Cycle Accelerated Aging Test (Automatic Boil Test) for Exterior Wet Use Wood Adhesives" D 3434 – 96, West Conshohocken, PA.

ASTM (1999) "Standard Specification for Adhesives for Structural Laminated Wood Products for Use Under Exterior (Wet Use) Exposure Conditions" D 2559-99, West Conshohocken, PA.

ASTM (1999) "Standard Test Methods for Evaluating Properties of Wood-Based and Particle Panel Materials" D 1037-99, West Conshohocken, PA.

ASTM (1998) "Standard Test Method for Strength Properties of Adhesive Bonds in Shear by Compression Loading" D 905-98, West Conshohocken, PA.

Bazan, I. M. M. (1980) "Ultimate bending strength of timber beams" PhD thesis, Nova Scotia Technical College, Halifax, Nova Scotia.

Buchanan, A., (1990) "Bending Strength of Lumber" Journal of Structural Engineering, 116(5), 1213-1229.

Canadian Highway Bridge Design Code, CAN/CSA-S6-00 (2000), Toronto, Ontario, Canada, CSA International.

Chen, Y., and Balaguru, P.N. (2003) "Design of fiber reinforced polymers (FRP) strengthened timber beams" Proceedings of the 48th International SAMPE Symposium, 2513-2524.

Cline, M., and Heim, A.L. (1912) "Tests of structural timbers" Tech. Bull., 108, Department of Agriculture, Forest Service, Washington, DC.

CSA Standard O86-01 (2001) Engineering Design in Wood, Toronto, Ontario, Canada, Canadian Standards Assiciation.

Davalos, J. F., Qiao, P. Z., and Trimble, B. S. (2000) "Fiber-Reinforced Composite and Wood Bonded Interfaces: Part 1. Durability and Shear Strength" Journal of composites Technology & Research, JCTRER, Vol. 22, No. 4, October 2000, 224-231.

Deppe, H. (1981) "Long-term comparative tests between natural and accelerated weathering exposures of coated and uncoated wood-based material" Proceedings of the Washington State University International Symposium on Particleboard, 79-100.

Foschi, R., and Barrett, J.D. (1977) "Longitudinal shear in wood beams; a design method" Canadian Journal of Civil Engineering, 4(3), 363-370.

Gentile, C., Svecova, D., and Rizkalla, S.H. (2002) "Timber Beams Strengthened with GFRP Bars: Development and Application" Journal of Composites for Construction, ASCE, 6(1), 11-20.

Hay, S., and Svecova, D. (2004) "Shear Strengthening of Timber Stringers Using GFRP Sheets" Thesis presented to the University of Manitoba, Winnipeg, Manitoba, Canada, in partial fulfillment of the requirements for the degree of Master of Science in Civil Engineering.

Hay, S., Thiessen, K., Svecova, D., and Backht, B. (2005) "The effectiveness of GFRP sheets for shear strengthening of timber" Submitted to ASCE Journal of Composites for Construction.

Herzog, B., Goodell, B., Lopez-Anido, R., Muszyñski, L, and Garder, D. (2004) "Effect of Creosote and Copper Naphthenate Preservative Treatments on Properties of FRP Composite Materials Used for Wood Reinforcement" Journal of Advanced Materials, Vol. 36, No. 4 October 2004, 25-33.

Huggins, M., Aplin, E., and Palmer, J.H. (1964) "Static and repeated load test of delaminated glulam beams". O.J.H.R.P. Rep. 32, Department of Civil Engineering, Toronto, Ontario.

Huggins, M., Palmer, J., and Aplin, E. (1966) "Evaluation of the Effect of Delamination" Engineering Journal, 49(2), 32-41.

ISIS Canada (2001) Design Manual No. 3 Reinforcing Concrete Structures with Fibre Reinforced Polymers. ISIS Canada, University of Manitoba, Winnipeg, Manitoba, Canada.

ISIS Canada (2001) Design Manual No. 4 Strengthening Reinforced Concrete Structures with Externally-Bonded Fibre Reinforced Polymers. ISIS Canada, University of Manitoba, Winnipeg, Manitoba, Canada.

Johns, K., and Lacroix, S. (2000) "Composite Reinforcement of Timber in Bending" Canadian Journal of Civil Engineering, 27, 899-906.

Keenan, F. J. (1974) "Shear strength of wood beams" Forest Products Journal, 24(9), 63-70.

Leicester, R.H. and Breitinger, H.O. (1992) "Measurement of shear strength" In. Proceedings, 1992 IUFRO S5.02 Timber Engineering Conference, Nancy, France, 287-299.

Lopez-Anido, R., Gardner, D., and Hensley, J. (2000) "Adhesive bonding of Eastern Hemlock glulam panels with E-glass/vinyl ester reinforcement" Forest Products Journal, Vol. 50, No. 11/12, 43-47.

Madsen, B. (1992) "Structural Behaviour of Timber". Timber Engineering Ltd. North Vancouver, British Columbia, Canada.

Markwardt, L.J. (1931) "The distribution and the mechanical properties of Alaska woods" Department of Agriculture, Forest Service, Tech. Bull., 226, Washington DC.

Mufti, A., Bakht, B., and Jaeger, L. (1996) "Bridge Superstructures-New Developments" National Book Foundation, Pakistan.

National Lumber Grades Authority (2002) "Standard Grading Rules for Canadian Lumber 2002" January 1, 2002 ed., New Westminster, British Columbia, Canada.

Newlin, J., Heck, G., and March, H. (1934) "New Method of Calculating Longitudinal Shear in Checked Wooden Beams" American Society of Mechanical engineers – Transactions, 56(10), 739-744.

Okkonen, E. A., and River, B. H. (1996) "Outdoor aging of wood-based panels and correlation with laboratory aging: Part 2", Forest Products Journal., Madison, Mar. 1996, Vol. 46, Iss. 3.

Plevris, N., and Triantafillou, T. (1992) "FRP-Reinforced Wood as Structural Material" Journal of Materials in Civil Engineering, ASCE, 4(3), 301-317.

Raknes, E. (1997) "Durability of structural wood adhesives after 30 years ageing" Holz als Roh- und Werkstoff; Holz Roh- Werkst., Vol. 55, No. 2, 83-90.

Rammer, D.R., Soltis, L. A., and Lebow, P. K. (1996) "Experimental shear Strength of Unchecked Solid-Sawn Douglas-Fir" Research paper FPL-RP-

553, Department of Agriculture, Forest Service, Forest Products Laboratory, Madison, WI.

Scoville, C. (2001), "Characterizing the Durability of PF and pMDI Adhesive Wood Composites Through Fracture Testing" , Ms.C. Thesis presented to the Virginia Polytechnic Institute and State University, Blacksburg, Virginia.

Soltis, L. A., and Gerhardt, T.D. (1988) "Shear design of wood beams: state of the art" Department of Agriculture, Forest Service, Forest Products Laboratory, FPL-GTR-56, Madison, WI.

Svecova, D., and Eden, R. (2004) "Flexural and shear strengthening of timber beams using glass fibre reinforced polymer bars – an experimental investigation" Canadian Journal of Civil Engineering, 31:45-55.

Tascioglu, C., Goodell, B., and Lopez-Anido, R. (2002) "Effects of wood-preservative treatments on mechanical properties of E-glass/Phenolic pultruded composite reinforcement for wood" Forest Products Journal, Mov/Dec 2002, Vol. 52, No. 11/12, 53-61.

Triantafillou, T. (1997) "Shear Reinforcement of Wood Using FRP Materials" Journal of Materials in Civil Engineering, ASCE, 9(2), 65-69.

Weibull, W. (1939) "A statistical theory of the strength of materials" Proc. No. 151, Royal Swedish Institute of Engineering Research, Stockholm, Sweden.

APENDIX A

DRAWINGS OF FRAME USED FOR DIRECT SHEAR TEST

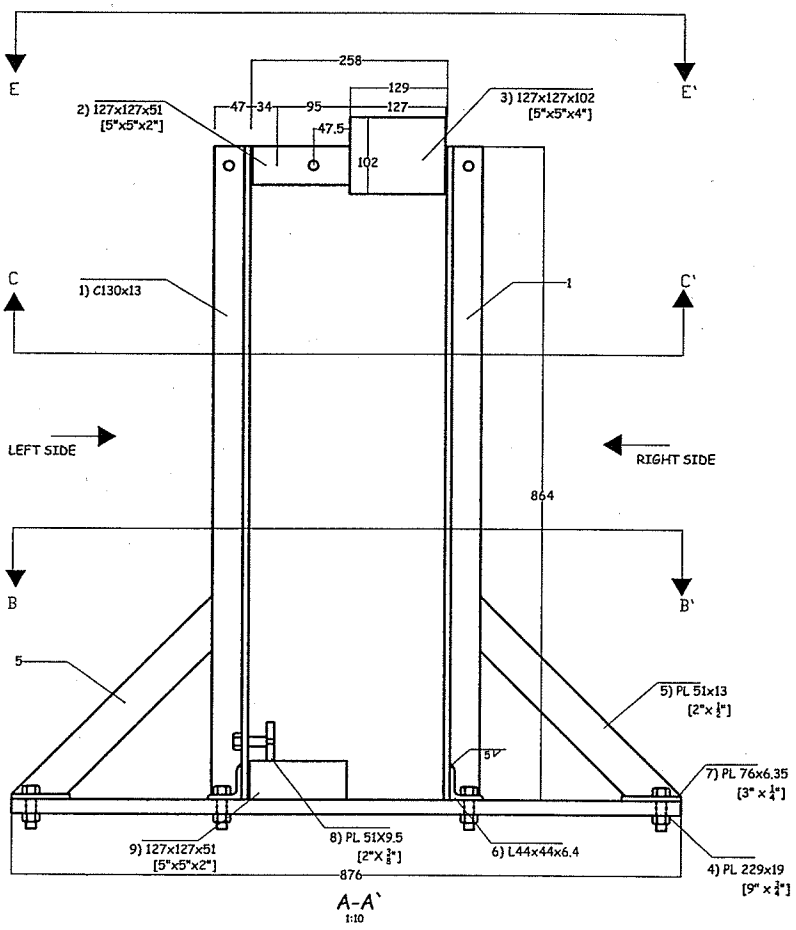

Figure A-1. Front view

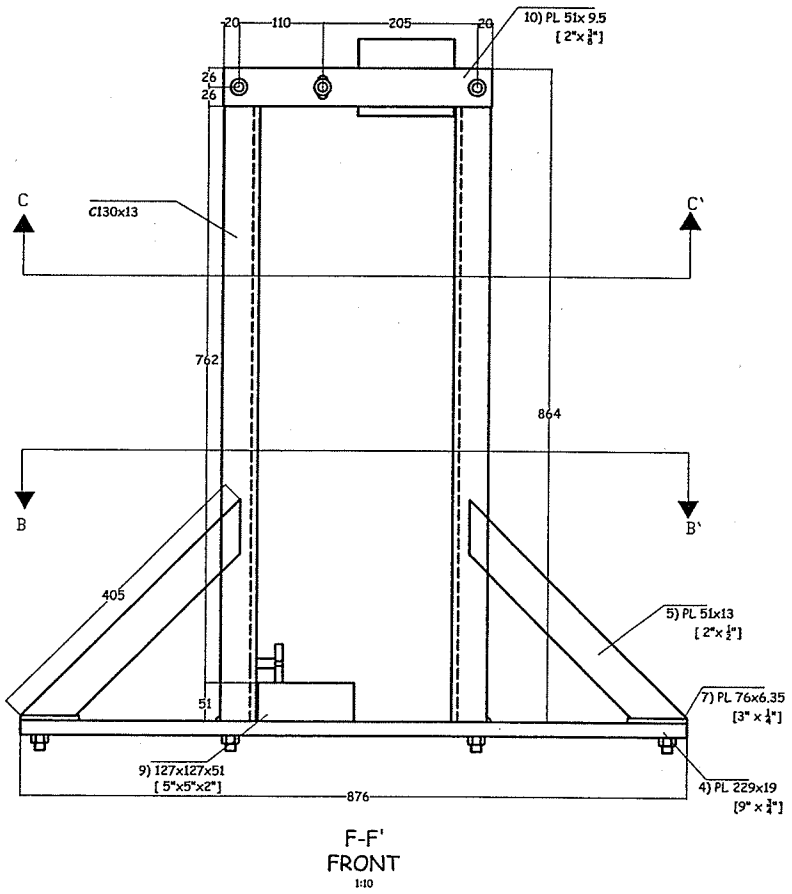

Figure A-2. Section F-F'

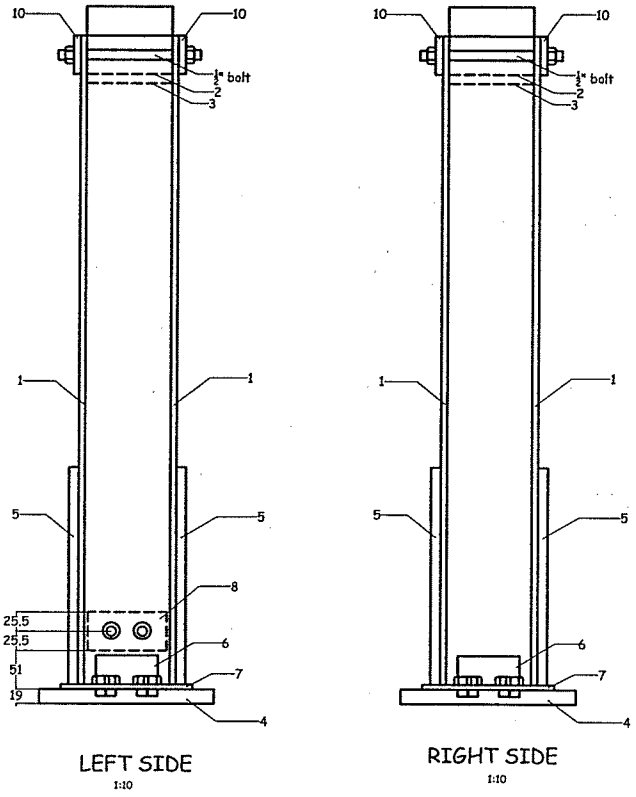

Figure A-3. Side views

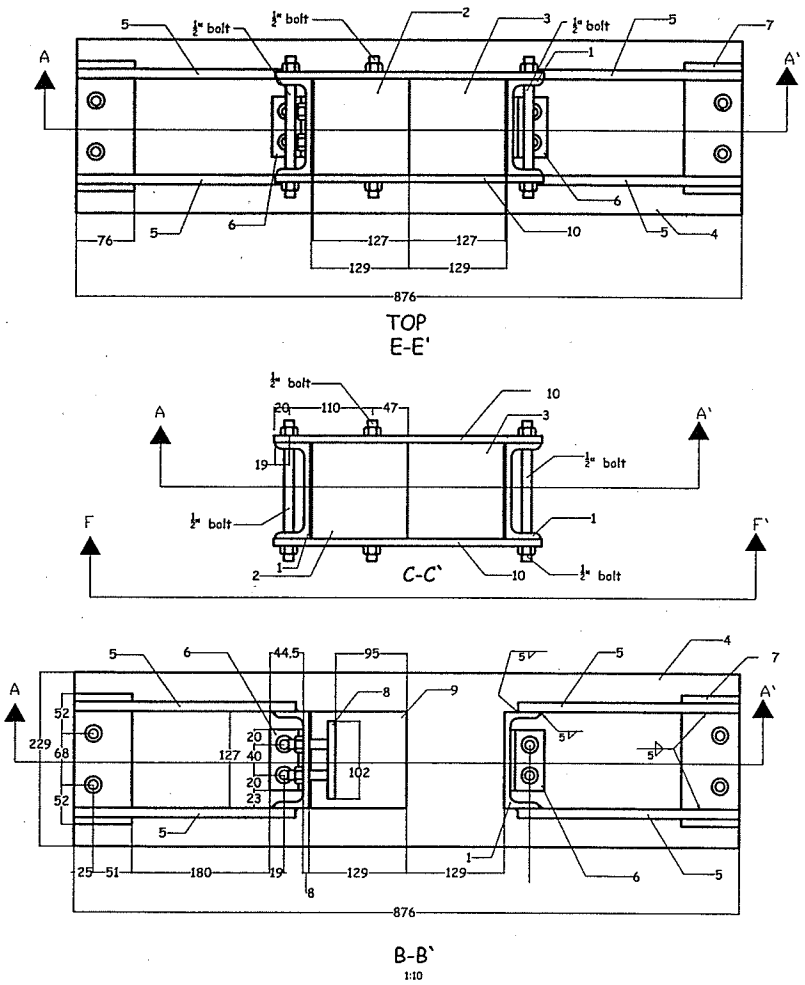

Figure A-4. Top views

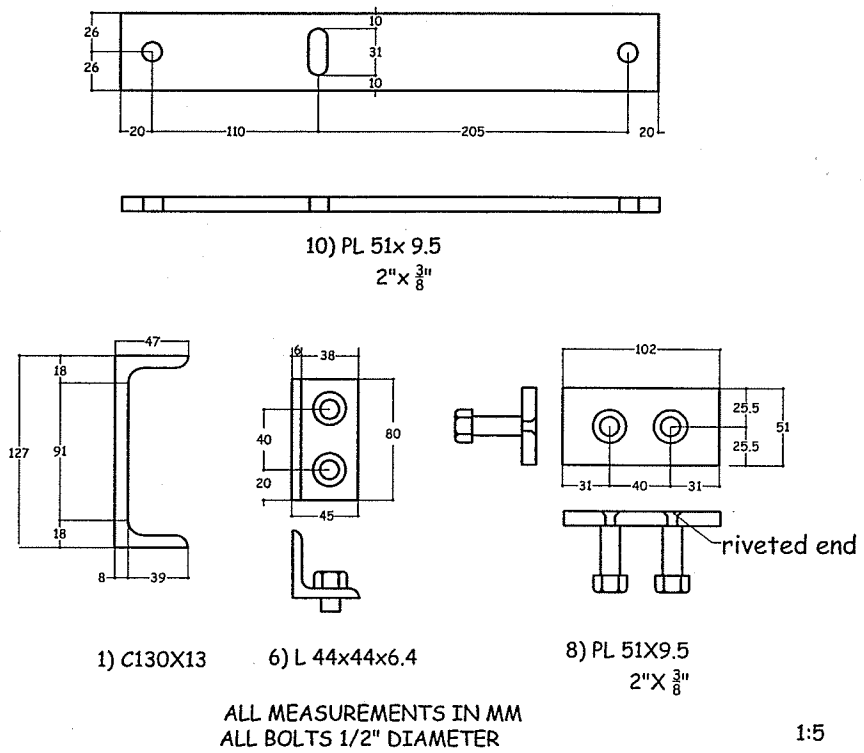

Figure A-5. Details